

GO BEYOND

Pioneers of omics webinar series

View recent webinar recordings about exciting
work at the forefront of omics research:

Artificial intelligence in proteomics

Presenters: Mathias Wilhelm, Martin Frejno, Karl Mechtler

Cancer research – towards personalized medicine

Presenters: Tami Geiger, Nicholas Rattray, Julio Sampaio

Biomarker discovery and validation of biological fluids

Presenters: Roland Bruderer, Chloé Jacquemin, Ivalya Roberts, Santosh D. Bhosale

Metabolomics approaches for systems biology

Presenters: Gunda Koellensperger, Evelyne Rampler, Cristina Coman,
Marina Wright Meulas, Tito Damiani

A new nano UHPLC for omics and biopharma (sessions in English and German)

Presenters: Nicola Berner, Karl Mechtler, Alexander Boychenko

Interactomics/Spatial omics

Presenters: Theodore Alexandrov, Manuel Matzinger, Alexey Chernobrovkin,
Alessandro Ori, Eneko Villanuev

Participation is free of charge. Sign-up now to view on-demand.
2022 sessions will be announced soon.

[Learn more](#)

thermo scientific

RESEARCH ARTICLE



WILEY

Isotopically characterised N₂O reference materials for use as community standards

Joachim Mohn¹ | Christina Biasi² | Samuel Bodé³ | Pascal Boeckx³ |
 Paul J. Brewer⁴ | Sarah Eggleston^{1,5} | Heike Geilmann⁶ | Myriam Guillevis^{1,7} |
 Jan Kaiser⁸ | Kristýna Kantnerová^{1,9} | Heiko Moossen⁶ | Joanna Müller^{1,10} |
 Mayuko Nakagawa¹¹ | Ruth Pearce⁴ | Isabell von Rein⁶ | David Steger¹ |
 Sakae Toyoda¹² | Wolfgang Wanek¹³ | Sarah K. Wexler⁸ |
 Naohiro Yoshida^{11,12} | Longfei Yu^{1,14}

¹Laboratory for Air Pollution/Environmental Technology, Empa, Dübendorf, Switzerland

²Department of Environmental and Biological Sciences, University of Eastern Finland, Kuopio, Finland

³Isotope Bioscience Laboratory – ISOFYS, Department of Green Chemistry and Technology, Faculty of Bioscience Engineering, Ghent University, Ghent, Belgium

⁴National Physical Laboratory, Middlesex, UK

⁵PAGES International Project Office, Bern, Switzerland

⁶Beutenberg Campus, Max-Planck-Institute for Biogeochemistry, Jena, Germany

⁷Air Pollution Control and Chemicals Division, Federal Office for the Environment, Bern, Switzerland

⁸Centre for Ocean and Atmospheric Sciences, School of Environmental Sciences, University of East Anglia, Norwich, UK

⁹Thermo Fisher Scientific, Bremen, Germany

¹⁰Plant Protection Chemistry, Agroscope, Wädenswil, Switzerland

¹¹Earth-Life Science Institute, Tokyo Institute of Technology, Tokyo, Japan

¹²Department of Chemical Science and Engineering, School of Materials and Chemical Technology, Tokyo Institute of Technology, Yokohama, Japan

¹³Terrestrial Ecosystem Research, Centre for Microbiology and Environmental Systems Science, University of Vienna, Vienna, Austria

¹⁴Institute of Environment and Ecology, Tsinghua Shenzhen International Graduate School (SIGS), Tsinghua University, Shenzhen, China

Correspondence

J. Mohn, Laboratory for Air Pollution/
Environmental Technology, Empa, Überlandstr.
129, 8600 Dübendorf, Switzerland.
Email: joachim.mohn@empa.ch

Funding information

EMPIR program co-financed by the Participating States and from the European Union's Horizon 2020 research and innovation program, Grant/Award Number: 16ENV06 Metrology for Stable Isotope Reference Standards (SIRS); H2020 Marie Skłodowska-Curie Actions, Grant/Award Number: EMPAPOSTDOCS-II; 754364; Japanese Swiss Science and Technology Program (JSPS International Fellowship for Research in Japan), Grant/Award Number: GR18108; Swiss National Science Foundation, Grant/Award Numbers: 200021_163075, 200021_166255

Rationale: Information on the isotopic composition of nitrous oxide (N₂O) at natural abundance supports the identification of its source and sink processes. In recent years, a number of mass spectrometric and laser spectroscopic techniques have been developed and are increasingly used by the research community. Advances in this active research area, however, critically depend on the availability of suitable N₂O isotope Reference Materials (RMs).

Methods: Within the project Metrology for Stable Isotope Reference Standards (SIRS), seven pure N₂O isotope RMs have been developed and their ¹⁵N/¹⁴N, ¹⁸O/¹⁶O, ¹⁷O/¹⁶O ratios and ¹⁵N site preference (SP) have been analysed by specialised laboratories against isotope reference materials. A particular focus was on the ¹⁵N site-specific isotopic composition, as this measurand is both highly diagnostic for source appointment and challenging to analyse and link to existing scales.

This is an open access article under the terms of the [Creative Commons Attribution](https://creativecommons.org/licenses/by/4.0/) License, which permits use, distribution and reproduction in any medium, provided the original work is properly cited.

© 2022 The Authors. *Rapid Communications in Mass Spectrometry* published by John Wiley & Sons Ltd.

[Correction added on 16 May 2022, after first online publication: CSAL funding statement has been added.]

Results: The established N₂O isotope RMs offer a wide spread in delta (δ) values: $\delta^{15}\text{N}$: 0 to +104‰, $\delta^{18}\text{O}$: +39 to +155‰, and $\delta^{15}\text{N}^{\text{SP}}$: −4 to +20‰. Conversion and uncertainty propagation of $\delta^{15}\text{N}$ and $\delta^{18}\text{O}$ to the Air-N₂ and VSMOW scales, respectively, provides robust estimates for $\delta^{15}\text{N}(\text{N}_2\text{O})$ and $\delta^{18}\text{O}(\text{N}_2\text{O})$, with overall uncertainties of about 0.05‰ and 0.15‰, respectively. For $\delta^{15}\text{N}^{\text{SP}}$, an offset of >1.5‰ compared with earlier calibration approaches was detected, which should be revisited in the future.

Conclusions: A set of seven N₂O isotope RMs anchored to the international isotope-ratio scales was developed that will promote the implementation of the recommended two-point calibration approach. Particularly, the availability of $\delta^{17}\text{O}$ data for N₂O RMs is expected to improve data quality/correction algorithms with respect to $\delta^{15}\text{N}^{\text{SP}}$ and $\delta^{15}\text{N}$ analysis by mass spectrometry. We anticipate that the N₂O isotope RMs will enhance compatibility between laboratories and accelerate research progress in this emerging field.

1 | INTRODUCTION

Since its first application by Sakae Toyoda and Naohiro Yoshida in 1999,¹ site-specific N₂O isotope analysis has been applied by many research groups to differentiate N₂O source and sink processes at different spatio-temporal scales (see reviews by Toyoda et al.,² Ostrom et al.,³ Decock et al.,⁴ Denk et al.,⁵ and Yu et al.⁶). Likewise, dual-isotope plots (e.g. $\delta^{15}\text{N}^{\text{SP}}/\delta^{15}\text{N}$) or so-called “isotope mapping” approaches have been used to constrain the contributions of specific pathways, and the effect of isotope fractionation during N₂O reduction.^{7,8} The informative value of N₂O isotope data has been markedly increased by using the data to inform biogeochemical models, providing regional and global patterns of N₂O losses and independent process information.^{9–12} Advances in applications have been accompanied and accelerated by progress in analytics, complementing the traditional high-precision isotope-ratio mass-spectrometry (IRMS)^{1,13} by laser spectroscopic techniques, with the potential for field applicability and real-time data coverage.^{14–19}

The isotopic composition of a sample is reported using the delta (δ) notation, which is the relative difference in isotope ratio (R) between a sample P and a reference material, i.e. $\delta(P/\text{ref}) = R_P/R_{\text{ref}} - 1$. For nitrogen, the $^{15}\text{N}/^{14}\text{N}$ isotope ratio is used, $R(^{15}\text{N}/^{14}\text{N}) = x(^{15}\text{N})/x(^{14}\text{N})$, where x is the isotopic abundance and tropospheric N₂ is the international reference material for the Air-N₂ scale. For oxygen, the $^{18}\text{O}/^{16}\text{O}$ and $^{17}\text{O}/^{16}\text{O}$ ratios are used, which are related to the Vienna Standard Mean Ocean Water (VSMOW) scale. In addition, we adopt the following notation conventions: $\delta^{15}\text{N} = \delta(^{15}\text{N}/^{14}\text{N}, P/\text{Air-N}_2)$ (average of both nitrogen atoms) and $\delta^{18}\text{O} = \delta(^{18}\text{O}/^{16}\text{O}, P/\text{VSMOW})$. The ^{15}N site preference (SP) is defined by the predominance of ^{15}N substitution in the central (α) position as compared to the terminal (β) position, and calculated accordingly as $\delta^{15}\text{N}^{\text{SP}} = \delta^{15}\text{N}^{\alpha} - \delta^{15}\text{N}^{\beta}$. All δ values in this paper are

reported against Air-N₂ (for $^{15}\text{N}/^{14}\text{N}$ ratios) and against VSMOW (for $^{18}\text{O}/^{16}\text{O}$ and $^{17}\text{O}/^{16}\text{O}$ ratios).

Further progress in N₂O isotope research critically depends on the compatibility of laboratory results.²⁰ To achieve this, individual laboratories have to implement a traceability chain, i.e. a hierarchy of reference materials which descends with increasing uncertainty, linking the isotopic composition of primary RMs used to realise the respective scale, through secondary standards and working laboratory standards to a sample.²¹ Generally, two RMs with distinct δ values should be used for calibration purposes, following the two-point data normalisation requirement. However, primary RMs and secondary scale anchors for $\delta^{15}\text{N}$ (ammonium sulfate, potassium nitrate) as well as $\delta^{17}\text{O}$ and $\delta^{18}\text{O}$ (water) have a different chemical identity than N₂O sample gas. Thus, a chemical conversion reaction²⁰ has to be implemented prior to analysis, which requires specialised laboratories.

The synthesis of N₂O by thermal decomposition of isotopically characterised ammonium nitrate (NH₄NO₃) has been suggested as an approach to link the position-dependent nitrogen isotopic composition of N₂O to the Air-N₂ scale.¹ The basic concept of this technique is that the nitrogen atom at the α -position of the formed N₂O originates from NO₃[−], while the β -nitrogen comes from NH₄⁺.²² The validity of the NH₄NO₃ decomposition technique has been confirmed,^{23,24} but its accuracy for the calibration of $\delta^{15}\text{N}^{\alpha}$ and $\delta^{15}\text{N}^{\beta}$ was found to be limited by non-quantitative NH₄NO₃ decomposition in combination with substantially different isotope enrichment factors of −4 or −19‰ for the conversion of the NO₃[−] or NH₄⁺ nitrogen atom into the α - or β -position of the N₂O molecule.²⁵ To overcome such difficulties, two new N₂O reference gases, USGS51 and USGS52, recently became available with assigned δ values based on a preliminary assessment by Naohiro Yoshida and Sakae Toyoda (Tokyo Institute of Technology).^{26,27} However, the two standards offer only a small range of $\delta^{15}\text{N}$ and $\delta^{18}\text{O}$ values (< 1‰), which is not suitable for a two-point calibration approach.

In the present study, we report the development of additional N_2O RMs within the framework of the European Metrology Programme for Innovation and Research (EMPIR) 16ENV06 project ‘Metrology for Stable Isotope Reference Standards (SIRS)’. The target isotopic composition of N_2O RMs was selected according to discussions at a stakeholder workshop at the 19th GGMT conference at Empa (29 August 2017).²⁸ The focus of this study is to extend the range of isotopic composition of N_2O RMs compared to RMs presented in Ostrom et al²⁶ and to provide additional $\delta^{17}\text{O}$ data in order to improve data quality/correction algorithms with respect to $\delta^{15}\text{N}^{\text{SP}}$ and $\delta^{15}\text{N}$ analysis by mass spectrometry. In addition, the link of δ values to the international isotope-ratio scales was revisited.

2 | EXPERIMENTAL

The main purpose of this study is the provision of isotopically characterised N_2O RMs, covering an extended range of delta values as compared to existing gases. Figure 1 provides a schematic overview on the links established within this study between existing international RMs and the novel gaseous N_2O RMs.

In section 2.1 (“left branch” of Figure 1), $^{15}\text{N}/^{14}\text{N}$ isotope ratios on the Air- N_2 scale were propagated from NH_4^+ and NO_3^- salts supplied by IAEA/USGS, through isotopic analysis of gravimetrically prepared NH_4NO_3 salts (section 2.1.2) and their thermal decomposition (section 2.1.3), to $\delta^{15}\text{N}^{\text{B}}(\text{N}_2\text{O})$ / $\delta^{15}\text{N}^{\text{A}}(\text{N}_2\text{O})$ in the novel

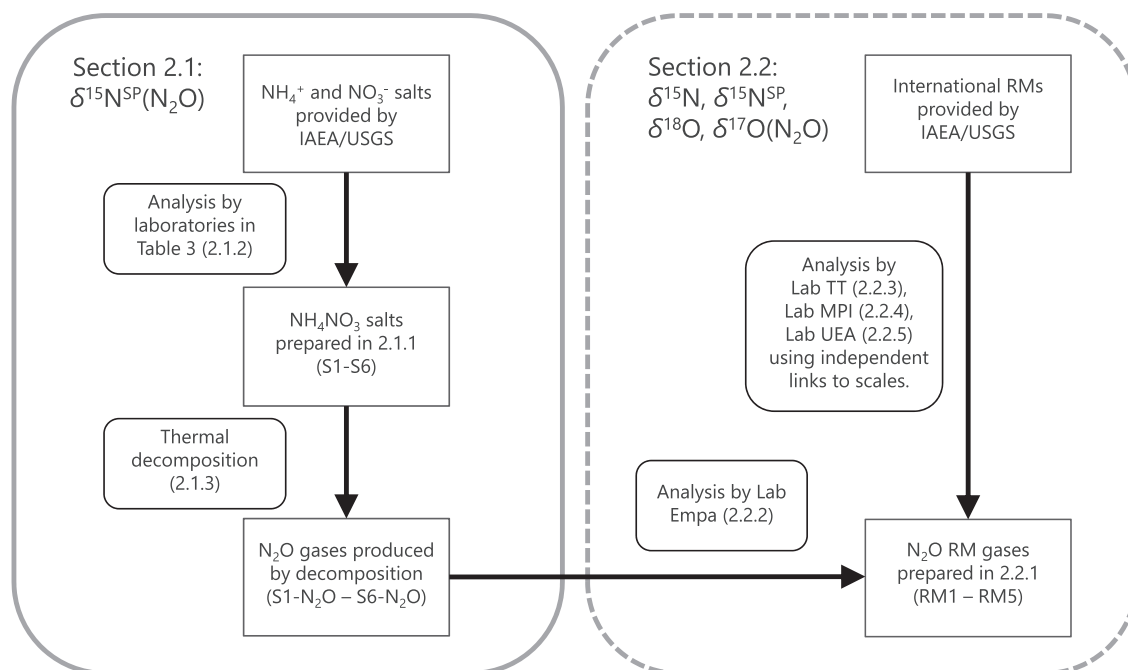


FIGURE 1 Schematic overview on the traceability chain applied in this study to propagate $^{15}\text{N}/^{14}\text{N}$, $^{18}\text{O}/^{16}\text{O}$ and $^{17}\text{O}/^{16}\text{O}$ isotope ratios from international RMs to $\delta^{15}\text{N}$, $\delta^{15}\text{N}^{\text{SP}}$, $\delta^{18}\text{O}$ and $\delta^{17}\text{O}$ in the novel N_2O RMs

TABLE 1 International RMs applied in this study for the analysis of $\delta^{15}\text{N}$ (NH_4NO_3 , $\delta^{15}\text{N}(\text{NH}_4^+)$ and $\delta^{15}\text{N}(\text{NO}_3^-)$ in NH_4NO_3 salts (section 2.1.2) and $\delta^{15}\text{N}$ as well as $\delta^{18}\text{O}$ in N_2O RMs (section 2.2). Values are taken from Brand et al²⁹ and Ostrom et al²⁶ and reported in ‰

		$\delta^{15}\text{N}_{\text{Air-N}_2}$	σ	$\delta^{18}\text{O}_{\text{VSMOW}}$	σ
IAEA-N-1	NH_4SO_4	+0.43	0.07	-	-
IAEA-N-2	NH_4SO_4	+20.41	0.12	-	-
USGS25	NH_4SO_4	-30.41	0.27	-	-
USGS26	NH_4SO_4	+53.75	0.24	-	-
IAEA-NO-3	KNO_3	+4.72	0.13	+13.2	-
USGS32	KNO_3	+180	0	+25.4	0.2
USGS34	KNO_3	-1.8	0.1	-27.78	0.37
USGS35	NaNO_3	+2.7	0.1	+56.81	0.31
USGS40	L-glutamic acid	-4.52	0.06	-	-
USGS51	N_2O	+1.21	0.21	+41.45	0.34
USGS52	N_2O	+0.29	0.25	+40.80	0.40

TABLE 2 Overview of NH_4NO_3 salts (S1–S6) prepared from commercially available NH_4NO_3 (A–E) and covering a wide range of $\delta^{15}\text{N}(\text{NH}_4^+)$ and $\delta^{15}\text{N}(\text{NO}_3^-)$ values

	Characteristic	A (unlabelled)	B ($^{15}\text{NH}_4\text{NO}_3$)	C ($\text{NH}_4^{15}\text{NO}_3$)	D ($^{15}\text{NH}_4^+$ -depleted)	E ($^{15}\text{NO}_3^-$ -depleted)
S1	Unlabelled NH_4NO_3	X				
S2	$^{15}\text{NH}_4$, $^{15}\text{NO}_3$ -low enriched	X	X	X		
S3	Ambient isotopic composition	X	X	X		
S4	$^{15}\text{NH}_4$, $^{15}\text{NO}_3$ -enriched	X	X	X		
S5	$^{15}\text{NH}_4$, $^{15}\text{NO}_3$ -high enriched	X	X	X		
S6	$^{15}\text{NH}_4$, $^{15}\text{NO}_3$ -depleted	X			X	X

N_2O RMs. The international RMs applied in this study are listed in Table 1. To provide a reliable link between the Air-N2 scale and the N_2O site-specific isotopic composition, the NH_4NO_3 decomposition reaction was optimised for high yield, reproducibility, and N_2O purity (see section 2.1.3). Following the recommended two-point calibration approach, a number of NH_4NO_3 salts, ranging from ^{15}N -depleted to ^{15}N -enriched, were prepared (see section 2.1.1), decomposed, and analysed.

In section 2.2 (“right branch” of Figure 1), preparation of N_2O RMs and analysis by expert laboratories for $\delta^{15}\text{N}(\text{N}_2\text{O})$, $\delta^{18}\text{O}(\text{N}_2\text{O})$, $\delta^{17}\text{O}(\text{N}_2\text{O})$ and $\delta^{15}\text{N}^{\text{SP}}(\text{N}_2\text{O})$ is described. In one laboratory (Empa), $\delta^{15}\text{N}^{\text{SP}}(\text{N}_2\text{O})$ in the N_2O RMs was linked to the Air-N2 scale making use of the traceability chain established in section 2.1. Links to scale applied in the other laboratories are independent and are described in detail in the respective experimental sections.

2.1 | Re-evaluation of NH_4NO_3 thermal decomposition technique to propagate $\delta^{15}\text{N}(\text{NO}_3^-)$ / $\delta^{15}\text{N}(\text{NH}_4^+)$ to $\delta^{15}\text{N}^{\alpha}(\text{N}_2\text{O})/\delta^{15}\text{N}^{\beta}(\text{N}_2\text{O})$

2.1.1 | Preparation of NH_4NO_3 salts

Six NH_4NO_3 salts (S1–S6), covering a wide range of $\delta^{15}\text{N}(\text{NH}_4^+)$ and $\delta^{15}\text{N}(\text{NO}_3^-)$ values, were produced by gravimetric mixing of five commercially available NH_4NO_3 salts (A–E). A: unlabelled NH_4NO_3 (purity >98%, K299.1, Carl Roth GmbH, Karlsruhe, Germany), B: $^{15}\text{NH}_4\text{NO}_3$ (>98% $^{15}\text{NH}_4^+$, NLM-711-1, Cambridge Isotope Laboratories Inc., Tewksbury, USA), C: $\text{NH}_4^{15}\text{NO}_3$ (>98% $^{15}\text{NO}_3^-$, NLM-712-1, Cambridge Isotope Laboratories Inc., Tewksbury, USA), D: $^{15}\text{NH}_4^+$ -depleted NH_4NO_3 (0.306% $^{15}\text{NH}_4^+$, Shoko Science Co., Ltd, Japan), E: $^{15}\text{NO}_3^-$ -depleted NH_4NO_3 (0.306% $^{15}\text{NO}_3^-$, Shoko Science Co., Ltd, Japan).

For preparation of these six NH_4NO_3 salts (Table 2), approximately 110 g of unlabelled NH_4NO_3 (A) was ground to a fine powder using a mortar and pestle and then dried at 120°C for 1 h (a temperature low enough to avoid triggering decomposition). From this, around 100 g (S1–S5) or around 40 g (S6) were gravimetrically (XP205, Mettler Toledo GmbH, Greifensee, Switzerland) mixed with appropriate amounts of salts B, C, D, and E to obtain the desired isotopic composition. The salt mixtures were dissolved in deionised

water (Milli-Q Advantage A10, Millipore AG, Switzerland), recrystallised, dried, and then stored in air-tight sample containers. The isotopic homogeneity of S1–S6 was confirmed by repeated IRMS analysis (MPI-BGC), demonstrating $\delta^{15}\text{N}(\text{NH}_4\text{NO}_3)$ values within <0.2‰ (σ , $n = 10$).

2.1.2 | Analysis of NH_4NO_3 salts for $\delta^{15}\text{N}$ (NH_4NO_3), $\delta^{15}\text{N}(\text{NH}_4^+)$ and $\delta^{15}\text{N}(\text{NO}_3^-)$ against IAEA and USGS RMs

Subsamples of the prepared NH_4NO_3 salts (S1–S6) were sent together with international reference materials ((NH_4)₂SO₄, NaNO₃, KNO₃) provided by the IAEA (International Atomic Energy Agency, Vienna, Austria) and by USGS (U.S. Geological Survey, Reston, USA) (Table 1) to eight isotope laboratories. Table 3 provides basic information on the analytical techniques applied by the laboratories. Details on the analytics are given in the supporting information (Supplementary Method 1).

$\delta^{15}\text{N}(\text{NH}_4\text{NO}_3)$, $\delta^{15}\text{N}(\text{NH}_4^+)$ and $\delta^{15}\text{N}(\text{NO}_3^-)$ results from all laboratories were calibrated using the provided international IAEA and USGS reference materials, with $\delta^{15}\text{N}$ values and uncertainties according to Brand et al.²⁹ and references cited therein. The uncertainty of laboratory results (σ_{cal}) was estimated from the uncertainty (σ_a , σ_b) in the linear calibration function (Equation 1), considering the uncertainty in IAEA and USGS standards and their analyses, as well as the uncertainty (σ_{meas}) in $\delta^{15}\text{N}_{\text{meas}}$, following the law of error propagation (Equation 2).^{39–41}

$$\delta^{15}\text{N}_{\text{cal}} = (a \pm \sigma_a) \delta^{15}\text{N}_{\text{meas}} + b \pm \sigma_b \quad (1)$$

$$\sigma_{\text{cal}} = \sqrt{(\sigma_a \delta^{15}\text{N}_{\text{meas}})^2 + (\sigma_{\text{meas}} a)^2 + \sigma_b^2} \quad (2)$$

Results ($\delta^{15}\text{N}_{\text{cal},i}$, $\sigma_{\text{cal},i}$) from individual laboratories i were combined to a weighted mean value ($\delta^{15}\text{N}_{\text{weighted}}$, Equation 3) with an uncertainty (σ_{weighted} , Equation 4)⁴²:

$$\delta^{15}\text{N}_{\text{weighted}} = \left[\frac{\delta^{15}\text{N}_{\text{cal},1}}{\sigma_{\text{cal},1}^2} + \frac{\delta^{15}\text{N}_{\text{cal},2}}{\sigma_{\text{cal},2}^2} + \dots \right] \times \sigma_{\text{weighted}}^2 \quad (3)$$

TABLE 3 Analytical techniques applied by the involved isotope laboratories for the analysis of $\delta^{15}\text{N}(\text{NH}_4\text{NO}_3)$, $\delta^{15}\text{N}(\text{NH}_4^+)$ and $\delta^{15}\text{N}(\text{NO}_3^-)$ in NH_4NO_3 salts (S1–S6). Details on the analytics are given in the supporting information (Supplementary Method 1)

Laboratory	Measurand	Technique
MPI-BGCLab (1)	$\delta^{15}\text{N}(\text{NH}_4\text{NO}_3)$	NH_4NO_3 analysis by elemental analyser (EA)/IRMS
UC DavisLab (2)	$\delta^{15}\text{N}(\text{NH}_4\text{NO}_3)$	NH_4NO_3 analysis by EA/IRMS
University of GhentLab (3)	$\delta^{15}\text{N}(\text{NH}_4\text{NO}_3)$	NH_4NO_3 analysis by EA/IRMS ³⁰
	$\delta^{15}\text{N}(\text{NH}_4^+)$	NH_4^+ oxidation with BrO^- to nitrite (NO_2^-), reaction with hydroxylamine (NH_2OH) to N_2O ; purge-and-trap (PT)-IRMS analysis ³¹
University of PittsburghLab (4)	$\delta^{15}\text{N}(\text{NO}_3^-)$	NO_3^- conversion into N_2O by denitrifier method; PT-IRMS analysis ^{32,33}
	$\delta^{15}\text{N}(\text{NH}_4\text{NO}_3)$	NH_4^+ oxidation with BrO^- to nitrite (NO_2^-), $\text{NO}_2^- + \text{NO}_3^-$ conversion into N_2O by denitrifier method; PT-IRMS analysis ³⁴
	$\delta^{15}\text{N}(\text{NO}_3^-)$	NO_3^- conversion into N_2O by denitrifier method; PT-IRMS analysis ^{32,33}
UEF-BGCLab (5)	$\delta^{15}\text{N}(\text{NH}_4^+)$	NH_3 microdiffusion on acid-impregnated glass fibre filter, followed by EA/IRMS analysis ³⁵
	$\delta^{15}\text{N}(\text{NO}_3^-)$	NO_3^- reaction with vanadium(III) chloride (VCl_3) and sodium azide (NaN_3) under acidic conditions to N_2O ; PT-IRMS analysis ³⁵
University of ViennaLab (6)	$\delta^{15}\text{N}(\text{NH}_4^+)$	NH_3 microdiffusion on acid-impregnated glass fibre filters, followed by EA/IRMS analysis ³⁵
	$\delta^{15}\text{N}(\text{NO}_3^-)$	NO_3^- reaction with VCl_3 and NaN_3 under acidic conditions to N_2O ; PT-IRMS analysis ³⁵
Tokyo Institute of TechnologyLab (7)	$\delta^{15}\text{N}(\text{NH}_4^+)$	NH_3 distillation into acid solution, NH_4^+ oxidation with KBrO to N_2 ; IRMS analysis ³⁶
	$\delta^{15}\text{N}(\text{NO}_3^-)$	After removal of NH_4^+ , NO_3^- reduction by Devarda's alloy to NH_4^+ and NH_3 distillation; IRMS analysis as above ³⁶
HydroisotopeLab (8)	$\delta^{15}\text{N}(\text{NH}_4^+)$	NH_4^+ oxidation with LiBrO to N_2 ; IRMS analysis
	$\delta^{15}\text{N}(\text{NO}_3^-)$	NH_4^+ removal by ion exchange; residual measured by EA/IRMS ^{37,38}

$$\sigma_{\text{weighted}} = 1 / \sqrt{\left(\frac{1}{\sigma_{\text{cal},1}}\right)^2 + \left(\frac{1}{\sigma_{\text{cal},2}}\right)^2 + \dots} \quad (4)$$

2.1.3 | NH_4NO_3 (S1–S6) thermal decomposition to N_2O (S1– N_2O –S6– N_2O)

Aliquots of approximately 1.0 g (12.5 mmol) of NH_4NO_3 salts (S1–S6) were weighed into round-bottomed glass flasks with a break-seal (150 mL, borosilicate glass, Willi Möller AG, Zürich, Switzerland). In a variant of the NH_4NO_3 decomposition reaction according to Szabó et al.,⁴³ 1.4 g NH_4HSO_4 (>99.99%, Art. No. 455849-100G, Sigma Aldrich GmbH, Buchs, Switzerland) and 0.2 g $(\text{NH}_4)_2\text{SO}_4$ (>99.5%, Art.

No. 09978-500G, Sigma Aldrich GmbH, Buchs, Switzerland) were added. Adding surplus NH_4^+ salt will lead to a loss in $\delta^{15}\text{N}^\beta$ information but was included to test if very high reaction yields can be achieved, which might still be attractive. Therefore, for S1, both variants (with/without $\text{NH}_4\text{HSO}_4/(\text{NH}_4)_2\text{SO}_4$) were tested, while for S2–S6 only decomposition without NH_4^+ addition was performed. Thereafter, the flasks were evacuated ($<10^{-1}$ mbar) and flame-sealed. The sealed flasks were placed in a circulating-air oven (model TSW 120 ED, Salvis AG, Reussbühl Switzerland) and heated to 270°C for 24 h.²⁵

After the decomposition reaction, the N_2O product gas, e.g. S1-derived- N_2O (here: S1- N_2O) or S6-derived- N_2O (S6- N_2O), was purified on a vacuum manifold by cryogenic distillation. Reaction by- and side-products (e.g. H_2O , HNO_3 , NH_3) were trapped at -78°C

(dry ice/ethanol bath); N_2O was trapped at -196°C (liquid N_2) in a coiled stainless-steel tube, while N_2 and O_2 (side products) were removed by evacuation with an oil-sealed rotary vane pump (RV3, Edwards Ltd, Crawley, UK). Thereafter, the N_2O product was condensed into 10 mL stainless-steel flasks (CS-20181323-ARBOR, ARBOR Fluidtec AG, Wohlen, Switzerland) under liquid-nitrogen cooling. The cryogenic extraction was repeated five times to fully capture the produced N_2O . Finally, the N_2O yield was determined gravimetrically (XP205 analytical balance, Mettler Toledo AG, Greifensee, Switzerland). The N_2O purity, i.e. the absence of IR-active impurities ($<5 \mu\text{mol mol}^{-1} \text{NO}$, $<1 \mu\text{mol mol}^{-1} \text{NO}_2$, and $<0.5 \mu\text{mol mol}^{-1} \text{NH}_3$), was confirmed by FTIR spectroscopy (Gasmeter CX4000 FTIR gas analyser, Temet Instruments Oy, Helsinki, Finland).⁴⁴ The distillation procedure (e.g. the trap size and the timing) was optimised for quantitative removal of N_2 ($<0.01\%$) and N_2O recovery ($>99.4\%$), using different gravimetric mixtures of high-purity N_2O and N_2 (Messer Schweiz, Lenzburg, Switzerland).

Test for consistency of NH_4NO_3 decomposition reaction

First, the consistency of the NH_4NO_3 decomposition reaction across the large range of δ values (^{15}N -depleted to highly ^{15}N -enriched in S1–S6 for both salts and N_2O) was tested. In detail, such tests were made by comparing $\delta^{15}\text{N}^\alpha$ of NH_4NO_3 -derived N_2O gases (S1- N_2O –S6- N_2O) with the $\delta^{15}\text{N}(\text{NO}_3^-)$ of substrate NH_4NO_3 salts (S1–S6) and $\delta^{15}\text{N}^\beta$ with $\delta^{15}\text{N}(\text{NH}_4^+)$, respectively. While the link provided by the NH_4NO_3 decomposition reaction was assumed to be valid across a wide range of δ values, the analytics involved in $\delta^{15}\text{N}^\alpha$, $\delta^{15}\text{N}^\beta$ or $\delta^{15}\text{N}(\text{NO}_3^-)$, $\delta^{15}\text{N}(\text{NH}_4^+)$ analysis might display non-linearities.

For this consistency test, the N_2O gases S2- N_2O , S3- N_2O , S5- N_2O and S6- N_2O were analysed together with S1- N_2O and S4- N_2O using the QCLAS analyser (section 2.2.2). S1- N_2O and S4- N_2O were selected as calibration gases, as they differ substantially in delta values ($>50\%$ in $\delta^{15}\text{N}$) and in preliminary experiments displayed a consistent offset between $\delta^{15}\text{N}^\alpha(\text{N}_2\text{O})$, $\delta^{15}\text{N}^\beta(\text{N}_2\text{O})$ and $\delta^{15}\text{N}(\text{NO}_3^-)$, $\delta^{15}\text{N}(\text{NH}_4^+)$ values (data not shown). For actual $\delta^{15}\text{N}^\alpha$ and $\delta^{15}\text{N}^\beta$ of S1- N_2O and S4- N_2O , known $\delta^{15}\text{N}(\text{NO}_3^-)$ and $\delta^{15}\text{N}(\text{NH}_4^+)$ values of the respective NH_4NO_3 salts were adopted and no correction for fractionation effects due to incomplete decomposition or branching isotope effects due to N_2 production was applied. The uncertainty of actual $\delta^{15}\text{N}^\alpha$ and $\delta^{15}\text{N}^\beta$ for S1- N_2O and S4- N_2O was estimated from the uncertainty of weighted mean $\delta^{15}\text{N}(\text{NO}_3^-)$ and $\delta^{15}\text{N}(\text{NH}_4^+)$ values (Table 5) and the standard deviation of $\delta^{15}\text{N}^\alpha$ and $\delta^{15}\text{N}^\beta$ analysis for repeated decomposition experiments using the law of error propagation.

Measured $\delta^{15}\text{N}^\alpha$ values of S1- N_2O and S4- N_2O and actual values, i.e. $\delta^{15}\text{N}(\text{NO}_3^-)$ of the educt NH_4NO_3 salts S1/S4, were used to define a linear calibration function (Equation 1). Then, $\delta^{15}\text{N}^\alpha_{\text{cal}}$ values were calculated from measured $\delta^{15}\text{N}^\alpha$ values of S2- N_2O , S3- N_2O , S5- N_2O and S6- N_2O using this correction function. The combined uncertainty in $\delta^{15}\text{N}^\alpha_{\text{cal}}$ values was calculated from the uncertainty in the actual $\delta^{15}\text{N}^\alpha$ values and the analyses of S1- N_2O and S4- N_2O , as well as the uncertainty in the measured $\delta^{15}\text{N}^\alpha$ of the N_2O gases S2- N_2O , S3- N_2O , S5- N_2O and S6- N_2O , in accordance with

Equation 2. Finally, the agreement of $\delta^{15}\text{N}^\alpha_{\text{cal}}$ values (Equation 1) of the individual N_2O gases (S1- N_2O –S6- N_2O) was tested against the actual $\delta^{15}\text{N}^\alpha$ values, i.e. the $\delta^{15}\text{N}(\text{NO}_3^-)$ of the respective NH_4NO_3 salts (S1–S6). The same procedure was applied to $\delta^{15}\text{N}^\beta$ and $\delta^{15}\text{N}(\text{NH}_4^+)$.

2.2 | Preparation of N_2O RMs and analysis for $\delta^{15}\text{N}(\text{N}_2\text{O})$, $\delta^{18}\text{O}(\text{N}_2\text{O})$, $\delta^{17}\text{O}(\text{N}_2\text{O})$ and $\delta^{15}\text{N}^{\text{SP}}(\text{N}_2\text{O})$

2.2.1 | Preparation of N_2O RMs

Currently available commercial N_2O gases offer only limited isotopic variability. Therefore, high-purity N_2O (99.999%, Linde, Germany) was supplemented with defined amounts of ^{15}N -enriched/ ^{15}N -depleted and ^{18}O -enriched N_2O dopant gas using a ten-port two-position valve (EH2C10WEPH, Valco Instruments Inc., Schenkon, Switzerland) with sample loops of different volumes (Table 4). The gas was transferred into evacuated Luxfer aluminium cylinders (3 L, 10 L, 20 L) with ROTAREX valves (Matar, Mazzano, Italy) to a final filling pressure below 45 bar to avoid condensation, given that the cylinder temperature remains above 15°C .

The dopant gases were commercial $^{15}\text{N}^{14}\text{NO}$ and $^{14}\text{N}^{15}\text{NO}$ (isotopic purity of $>98\%$, Cambridge Isotope Laboratories Inc., Tewksbury, USA), as well as ^{18}O -enriched N_2O ($(36.25 \pm 0.10)\%$ NN^{16}O , $(63.75 \pm 0.76)\%$ NN^{18}O) and $^{15}\text{N}^\beta$ -depleted N_2O ($\delta^{15}\text{N}^\alpha = (-2.54 \pm 0.005)\%$, $\delta^{15}\text{N}^\beta = (-16.221 \pm 0.03)\%$, $\delta^{18}\text{O} = (+38.92 \pm 0.003)\%$), both produced and characterised at Empa. Details on the production and analysis of ^{18}O -enriched N_2O and $^{15}\text{N}^\beta$ -depleted N_2O are provided in the supporting information (Supplementary Method 2). N_2O RMs were provided to laboratories in 50 mL (Lab TT, Lab UEA) or 150 mL (Lab MPI) stainless-steel flasks (CS-07291113-ARBOR, Arbor Fluidtec AG, Wohlen, Switzerland) for isotopic analysis.

2.2.2 | Analysis of N_2O RMs for $\delta^{15}\text{N}^\alpha$ and $\delta^{15}\text{N}^\beta$ by QCLAS at Empa (Lab Empa)

For analysis of $\delta^{15}\text{N}^\alpha$, $\delta^{15}\text{N}^\beta$ and $\delta^{18}\text{O}$ in the N_2O gases, a QCLAS spectrometer (Aerodyne Research Inc., Billerica, MA, USA)⁴⁵ equipped with a continuous-wave quantum cascade laser (cw-QCL) with spectral emission at 2203 cm^{-1} and an astigmatic Herriott multi-pass absorption cell (204 m path length) was applied. Prior to analysis, pure N_2O gases (e.g. RM1–RM6, S1- N_2O –S6- N_2O) were diluted to around $50 \mu\text{mol mol}^{-1}$ using one cylinder of synthetic air ($(20.5 \pm 0.5)\%$ O_2 in N_2 , Messer Schweiz AG, Switzerland) into 2 L high-pressure stainless-steel cylinders (Luxfer, Messer Schweiz AG, Switzerland) using a ten-port two-position valve (EH2C10WEPH with a 1 mL sample loop, Valco Instruments Inc., Schenkon, Switzerland). A singular cylinder of synthetic air was used for all experiments to minimise differences in the oxygen content, which would otherwise affect pressure broadening of absorption lines, result in differences in apparent

TABLE 4 Overview of N₂O RMs produced from high-purity N₂O supplemented with ¹⁵N-enriched/¹⁵N-depleted and ¹⁸O-enriched N₂O

	Characteristic	High-purity N ₂ O	¹⁵ N ¹⁴ NO	¹⁴ N ¹⁵ NO	NN ¹⁸ O	¹⁵ N ^β -depl. N ₂ O
RM1A/RM1B	High-purity N ₂ O	X				
RM2	Ambient isotopic composition	X		X	X	X
RM3A/RM3B	¹⁵ N-/ ¹⁸ O-enriched; no SP	X	X	X	X	
RM4	¹⁵ N-/ ¹⁸ O-highly enriched; no SP	X	X	X	X	
RM5	¹⁵ N-enriched; SP	X	X	X		

isotopologue mole fractions and increase uncertainties. The selection of synthetic air as diluent is somewhat arbitrary and not meant to represent an alternative for a full-air matrix for high-accuracy ambient N₂O isotope analysis, which would enclose noble and trace gases depending on the analytics and accuracy requirements.

The spectroscopically determined isotope ratios were related to the isotope-ratio scales realised by Toyoda et al.¹ through the analysis of calibration gases CG1 ($\delta^{15}\text{N}^\alpha = (+25.73 \pm 0.24)\text{‰}$, $\delta^{15}\text{N}^\beta = (+25.44 \pm 0.36)\text{‰}$, $\delta^{18}\text{O} = (+35.86 \pm 0.22)\text{‰}$) and CG2 ($\delta^{15}\text{N}^\alpha = (-48.59 \pm 0.25)\text{‰}$, $\delta^{15}\text{N}^\beta = (-46.11 \pm 0.43)\text{‰}$, $\delta^{18}\text{O} = (+27.37 \pm 0.11)\text{‰}$). The isotopic composition of the calibration gases had been previously analysed by Sakae Toyoda at the Tokyo Institute of Technology using their analytical technique as a link to the international scales.

For the analysis of N₂O RMs by QCLAS, the site-specific isotopic information provided by NH₄NO₃-derived N₂O gases S1-N₂O ($\delta^{15}\text{N}^\alpha = (-1.41 \pm 0.21)\text{‰}$, $\delta^{15}\text{N}^\beta = (+0.33 \pm 0.12)\text{‰}$) and S4-N₂O ($\delta^{15}\text{N}^\alpha = (+52.36 \pm 0.15)\text{‰}$, $\delta^{15}\text{N}^\beta = (+53.06 \pm 0.16)\text{‰}$) was propagated to the N₂O RMs (RM1–RM5). For this, the N₂O RMs were analysed together with S1-N₂O and S4-N₂O, as described in the preceding section, to propagate the moiety-specific isotopic composition defined by S1 and S4 to the novel RMs (Equation 1). An uncertainty assessment was conducted according to Equation 2 including uncertainties of S1-N₂O and S4-N₂O, as discussed above, their analyses, and the analyses of RMs.

2.2.3 | Analysis of N₂O RMs for $\delta^{15}\text{N}^\alpha$, $\delta^{15}\text{N}^\beta$ and $\delta^{18}\text{O}$ by DI-IRMS and $\delta^{17}\text{O}$ by HR-IRMS at Tokyo Institute of Technology (Lab TT)

N₂O RMs were analysed for $\delta^{15}\text{N}$, $\delta^{15}\text{N}^\alpha$, $\delta^{15}\text{N}^\beta$, $\delta^{18}\text{O}$ and $\delta^{15}\text{N}^{\text{SP}}$ values with a dual-inlet (DI) MAT 252 mass spectrometer (Thermo Fisher Scientific, Bremen, Germany) against an isotopically characterised laboratory tank of pure N₂O (N₂O-5N, Showa Denko, >99.999% chemical purity); C1: $\delta^{15}\text{N} = (-2.4 \pm 0.4)\text{‰}$, $\delta^{15}\text{N}^\alpha = (-4.5 \pm 0.4)\text{‰}$, $\delta^{15}\text{N}^\beta = (-0.3 \pm 0.8)\text{‰}$, $\delta^{18}\text{O} = (+23.3 \pm 1.2)\text{‰}$. IRMS analysis of the N₂O intramolecular ¹⁵N distribution was based on the quantification of the fragment NO⁺ (*m/z* 30 and 31) and molecular N₂O⁺ (*m/z* 44, 45 and 46) ions to calculate isotope ratios for the entire molecule and the central (α) and terminal (β) N atom. Analysis of $\delta^{15}\text{N}$ (45/44) and $\delta^{15}\text{N}^\alpha$ involves correction for interfering ¹⁴N₂¹⁷O⁺ (*m/z* 45) and ¹⁴N¹⁷O⁺ (*m/z* 31) using actual $\Delta^{17}\text{O}$ values

analysed at the University of East Anglia (UEA). For the analysis of $\delta^{15}\text{N}^\alpha$ and $\delta^{15}\text{N}^\beta$, rearrangement of N atoms (N^α and N^β) in the ion source was considered. The $\delta^{15}\text{N}$, $\delta^{15}\text{N}^\alpha$ and $\delta^{15}\text{N}^\beta$ values of the local reference gas were previously anchored to Air-N₂ by NH₄NO₃ decomposition,¹ whereas the $\delta^{18}\text{O}$ value was anchored to VSMOW by converting N₂O into CO₂ with graphite and a platinum foil (Yoshida, unpublished data). The analytical uncertainties were calculated from the uncertainty of the in-house working N₂O standard gases and the standard deviation for repeated measurements of the sample gas (N₂O RM) and the in-house working N₂O standard following the law of error propagation. Specifically, the uncertainty of the in-house working N₂O standard gas for $\delta^{15}\text{N}$, $\delta^{15}\text{N}^\alpha$ and $\delta^{15}\text{N}^\beta$ values comprises both the uncertainty in the $\delta^{15}\text{N}(\text{NH}_4^+)$ and $\delta^{15}\text{N}(\text{NO}_3^-)$ analysis and the repeatability of the NH₄NO₃ decomposition reaction. For $\delta^{18}\text{O}$, the uncertainty of the in-house working N₂O standard gas includes the repeatability of the conversion reaction of N₂O into CO₂ with graphite. $\delta^{17}\text{O}$ signatures of three N₂O RMs (RM1A, RM3A, RM4) were analysed by high-resolution IRMS (MAT 253 Ultra, Thermo Scientific, Bremen, Germany). Experimental details of this prototype analyses are provided in the supporting information (Supplementary Method 3).

2.2.4 | Analysis of N₂O RMs for $\delta^{15}\text{N}$ and $\delta^{18}\text{O}$ by EA/IRMS and DI-IRMS at MPI-BGC (Lab MPI)

Analysis for $\delta^{15}\text{N}$ by EA/IRMS (MPI-I)

$\delta^{15}\text{N}$ values of the N₂O RMs were determined using a modified EA/IRMS system (EA 1110 CHN combustion analyzer, CE Instruments Ltd, Wigan, UK; Delta plus isotope ratio mass spectrometer, Thermo Fisher Scientific, Bremen, Germany). The system and the method used have been described by Sperlich et al.⁴⁶ The $\delta^{15}\text{N}$ values of the sample N₂O were scaled to IAEA-N-1 and USGS32. In addition to the sample gases, an in-house standard N₂O gas NINO was analysed in each sample run, which was used as an anchor for $\delta^{15}\text{N}$ measurements by DI-IRMS. USGS40, and the in-house standards Ali-j3 ($\delta^{15}\text{N} = (-1.51 \pm 0.1)\text{‰}$; acetic anilide) and Caf-j3 ($\delta^{15}\text{N} = (-15.46 \pm 0.1)\text{‰}$; caffeine), were analysed in each daily run as quality controls, but not used for data correction.

Analysis for $\delta^{15}\text{N}$ and $\delta^{18}\text{O}$ by dual-inlet IRMS (MPI-II)

The N₂O RMs were analysed twice (September 2019, February 2021) on a DI-IRMS system (MAT253, Thermo Fisher Scientific, Bremen,

Germany) using separately subsampled flasks. We note that the published δ values for USGS51 and USGS52 are average values with a rather large deviation between laboratories. Therefore, we scaled the DI-IRMS $\delta^{15}\text{N}$ analyses to the in-house standard NINO using the value reported for the primary calibration using EA/IRMS ($\delta^{15}\text{N} = (+0.54 \pm 0.21)\text{‰}$). The $\delta^{18}\text{O}$ value of NINO ($\delta^{18}\text{O} = (+39.94 \pm 0.34)\text{‰}$) was determined by setting the $\delta^{18}\text{O}$ of USGS51 equal to the average value from the interlaboratory comparison ($\delta^{18}\text{O} = (+41.45 \pm 0.34)\text{‰}$) published by Ostrom et al.²⁶ In addition, USGS52 was analysed to test the consistency of the results (shown in Table 9) but not used for correction.

In contrast to the EA/IRMS technique, where $\delta^{15}\text{N}$ is measured from N_2 gas, the DI-IRMS method allows the analyses of $\delta^{15}\text{N}$ and $\delta^{18}\text{O}$ values by simultaneously recording m/z 44 ($^{14}\text{N}^{14}\text{N}^{16}\text{O}^+$), 45 ($^{15}\text{N}^{14}\text{N}^{16}\text{O}^+$, $^{14}\text{N}^{15}\text{N}^{16}\text{O}^+$, $^{14}\text{N}^{14}\text{N}^{17}\text{O}^+$) and 46 ($^{14}\text{N}^{14}\text{N}^{18}\text{O}^+$, $^{15}\text{N}^{15}\text{N}^{16}\text{O}^+$, $^{14}\text{N}^{15}\text{N}^{17}\text{O}^+$) ion currents. $\delta^{15}\text{N}$ and $\delta^{18}\text{O}$ values for N_2O RMs were calculated according to Kaiser et al.⁴⁷ to correct for isobaric interferences, for which the $\Delta^{17}\text{O}$ values determined by UEA were used.

The uncertainty of the analyses was calculated from the uncertainty of $\delta^{15}\text{N}$ and $\delta^{18}\text{O}$ measurements of the N_2O standard gases (NINO, USGS51) and from the standard deviation for repeated measurements of the sample gas (N_2O RM) and the N_2O standards, following the law of error propagation.

2.2.5 | Analysis of N_2O RMs for $\delta^{15}\text{N}$, $\delta^{18}\text{O}$ and $\delta^{17}\text{O}$ by IRMS at UEA (Lab UEA)

Analysis for $\delta^{15}\text{N}$, $\delta^{18}\text{O}$ and $\delta^{17}\text{O}$ by GC/IRMS (UEA-I)

The N_2O RM samples and a N_2O -MG-6.0 working reference (99.9999% chemical purity, N_2O -MG-6.0, Messer-Griesheim, Krefeld, Germany) were diluted to $0.09 \text{ mmol mol}^{-1}$ in N_2 (zero grade, BOC, UK), filled into 20 mL serum vials (Wheaton, Fisher Scientific, Loughborough, UK) and analysed for $^{45}\delta(\text{N}_2\text{O})$ and $^{46}\delta(\text{N}_2\text{O})$ on a custom-built automated cryogenic extraction and purification system comprised of an autosampler, a valve system, and PoraPLOT Q pre- and main columns (Agilent Technologies, Santa Clara, USA), coupled to a GEO 20-20 isotope ratio mass spectrometer (Sercon Ltd, Crewe, UK).

Using the same mass spectrometer, these samples were also analysed for $^{33}\delta(\text{O}_2) = \delta^{17}\text{O}$, $^{34}\delta(\text{O}_2) \approx \delta^{18}\text{O}$ (the error of this approximation is $<0.01\text{‰}$) and $^{29}\delta(\text{N}_2) = \delta^{15}\text{N}$ after cryogenic N_2O extraction and decomposition to N_2 and O_2 with a 500 mm long pure gold tube (1.6 mm OD, 0.6 mm ID; Heimerle & Meule, Pforzheim, Germany) held at 854°C . N_2 and O_2 were separated directly (without further cryofocussing) on a molecular-sieve 5-Å PLOT main column (Restek, Bellefonte, USA, $30 \text{ m} \times 0.32 \text{ mm}$, $30 \mu\text{m}$, 30°C , 1.3 mL min^{-1} (at 20°C and 1 bar, standard temperature and pressure)). The quantitative conversion of N_2O was verified by swapping the molecular-sieve main column for the PoraPLOT Q main column and testing for residual N_2O with the mass spectrometer. The raw $\delta^{17}\text{O}$ and $\delta^{18}\text{O}$ measurements were affected by scale compression. To correct for this, a logarithmic scale normalisation^{48,49}

was applied using the $\delta^{18}\text{O}$ value of $+112.4\text{‰}$ (relative to N_2O -MG-6.0) derived from the $^{46}\delta(\text{N}_2\text{O})$ measurements of the diluted RM4 sample measured on the GEO 20-20 mass spectrometer. The same normalisation was used for $\delta^{17}\text{O}$ as for $\delta^{18}\text{O}$ because no N_2O reference material with a calibrated $\delta^{17}\text{O}$ value was available. No scale-normalisation was applied to the $\delta^{15}\text{N}$ measurements. Uncertainties were calculated using the law of error propagation from the standard deviations of replicate measurements against the working reference gas and the calibration uncertainties of the working reference gas against Air- N_2 and VSMOW.⁴²

Analysis for $\delta^{15}\text{N}$, $\delta^{18}\text{O}$ and $\delta^{17}\text{O}$ by dual-inlet IRMS (UEA-II)

The N_2O RM samples were analysed for $^{45}\delta(\text{N}_2\text{O})$ and $^{46}\delta(\text{N}_2\text{O})$ with respect to the N_2O working reference N_2O -MG-6.0 using the dual-inlet system of a Finnigan MAT 253 isotope ratio mass spectrometer (Thermo Fisher Scientific, Bremen, Germany). The N_2O -MG-6.0 working reference has been calibrated by Kaiser et al.,⁵⁰ who reported values of $\delta^{15}\text{N} = (+1.01 \pm 0.06)\text{‰}$ with respect to Air- N_2 , as well as $\delta^{18}\text{O} = (+38.45 \pm 0.22)\text{‰}$ and $\delta^{17}\text{O} = (+19.66 \pm 0.11)\text{‰}$ with respect to VSMOW.⁵¹ Actual $\delta^{17}\text{O}$ values of N_2O RMs analysed with the Sercon GEO 20-20 were used for the data correction according to Kaiser et al.⁴⁷ Uncertainties were calculated using the law of error propagation from the standard deviations of replicate measurements against the working reference gas and the calibration uncertainties of the working reference gas against Air- N_2 and VSMOW.³⁰

3 | RESULTS AND DISCUSSION

3.1 | Re-evaluation of the NH_4NO_3 thermal decomposition technique to propagate $\delta^{15}\text{N}(\text{NO}_3^-)/\delta^{15}\text{N}(\text{NH}_4^+)$ to $\delta^{15}\text{N}^\alpha(\text{N}_2\text{O})/\delta^{15}\text{N}^\beta(\text{N}_2\text{O})$

In the following sections, the main procedures for anchoring of $\delta^{15}\text{N}^\alpha$ and $\delta^{15}\text{N}^\beta$ in N_2O to the Air- N_2 scale and calculating uncertainties are described. Section 3.1.1 details results of $\delta^{15}\text{N}(\text{NH}_4^+)$ and $\delta^{15}\text{N}(\text{NO}_3^-)$ analyses in NH_4NO_3 salts (S1–S6) by eight isotope laboratories against international IAEA and USGS standards. Section 3.1.2 informs about optimal conditions for NH_4NO_3 decomposition at high yield, repeatability, and N_2O purity. To enable the two-point calibration, a number of NH_4NO_3 salts with different isotopic composition were produced and decomposed and the consistency of $\delta^{15}\text{N}^\alpha$ and $\delta^{15}\text{N}^\beta$ of the N_2O gases (S1- N_2O –S6- N_2O) and the $\delta^{15}\text{N}(\text{NH}_4^+)$ and $\delta^{15}\text{N}(\text{NO}_3^-)$ of NH_4NO_3 salts (S1–S6) was tested (section 3.1.3).

3.1.1 | Isotopic composition of NH_4NO_3 salts for $\delta^{15}\text{N}(\text{NH}_4\text{NO}_3)$, $\delta^{15}\text{N}(\text{NO}_3^-)$ and $\delta^{15}\text{N}(\text{NH}_4^+)$

The isotopic composition of the prepared NH_4NO_3 salts (S1–S6), as analysed by the eight isotope laboratories and calibrated to Air- N_2 by analysis of IAEA and USGS standards, is indicated in Table 5. The

TABLE 5 $\delta^{15}\text{N}(\text{NH}_4\text{NO}_3)$ (top), $\delta^{15}\text{N}(\text{NO}_3^-)$ (middle), and $\delta^{15}\text{N}(\text{NH}_4^+)$ (bottom) of prepared NH_4NO_3 salts (S1–S6) analysed by different laboratories using techniques described in Table 3 and the supporting information (Supplementary Method 1). Results from individual laboratories were calibrated using international (IAEA, USGS) standards²⁹ and their uncertainties (σ) calculated following the law of error propagation. Laboratories: (1) MPI-BGC, (2) UC Davis, (3) University of Ghent, (4) University of Pittsburgh, (5) UEF-BGC, (6) University of Vienna, (7) Tokyo Tech, (8) Hydroisotop

$\delta^{15}\text{N}(\text{NH}_4\text{NO}_3)/\text{‰}$	Lab (1)	Lab (2)	Lab (3)	Lab (4) ^a			σ (1)	σ (2)	σ (3)	σ (4) ^a			Weighted mean $\pm \sigma$
S1	−0.60	−0.70	+0.05	+0.64			0.11	0.07	0.09	0.08			−0.44 \pm 0.05
S2	+13.77	+13.73	+14.48	+15.11			0.17	0.15	0.10	0.07			+14.14 \pm 0.08
S3	+7.23	+7.02	+8.11	+8.22			0.13	0.07	0.11	0.06			+7.31 \pm 0.06
S4	+52.65	+52.42	+53.27	+54.55			0.17	0.41	0.24	0.11			+52.81 \pm 0.13
S5	+107.56	+107.61	+108.21	+110.58			0.24	0.32	0.19	0.18			+107.90 \pm 0.13
S6	−49.91	−50.00	−49.37	−49.25			0.13	0.14	0.24	0.13			−49.87 \pm 0.09
$\delta^{15}\text{N}$ (NO_3^-)/‰	Lab (3)	Lab (4)	Lab (5)	Lab (6)	Lab (7)	Lab (8)	σ (3)	σ (4)	σ (5)	σ (6)	σ (7)	σ (8)	Weighted mean $\pm \sigma$
S1	−2.07	−0.78	−1.76	−1.27	−1.36	−0.09	0.23	0.66	0.70	0.13	0.14	1.03	−1.41 \pm 0.09
S2	+12.95	+13.80	+13.57	+13.75	+13.25	+16.13	0.22	0.09	0.69	0.14	0.37	1.04	+13.69 \pm 0.07
S3	+13.41	+14.23	+14.04	+14.15	+12.48	+15.73	0.24	0.13	0.69	0.14	0.51	1.04	+14.04 \pm 0.09
S4	+52.03	+53.11	+53.03	+51.60	+51.79	+54.69	0.51	0.10	0.83	0.26	0.09	1.08	+52.36 \pm 0.07
S5	+112.78	+114.33	+114.86	+114.42	+112.02	+117.50	1.67	0.16	1.42	0.39	2.30	1.24	+114.37 \pm 0.15
S6	−51.44	−50.54	−51.07	−50.64	−50.37	−48.48	0.46	0.14	0.94	0.34	0.11	1.07	−50.47 \pm 0.08
$\delta^{15}\text{N}$ (NH_4^+)/‰	Lab (3)	Lab (5)	Lab (6)	Lab (7)	Lab (8)		σ (3)	σ (5)	σ (6)	σ (7)	σ (8)		Weighted mean $\pm \sigma$
S1	+0.21	+1.02	+0.15	+0.96	+1.12		0.59	0.35	0.10	0.23	0.70		+0.33 \pm 0.09
S2	+13.59	+14.72	+13.97	+14.99	+15.65		1.18	0.58	0.15	0.28	0.72		+14.26 \pm 0.13
S3	+0.19	+1.31	+0.14	+0.74	+0.71		0.77	0.45	0.08	0.97	0.70		+0.19 \pm 0.08
S4	+52.85	+52.17	+52.32	+53.14	+53.34		1.01	1.36	0.27	0.09	0.91		+53.06 \pm 0.08
S5	+99.18	+100.35	+101.43	+102.82	+100.08		1.40	1.08	0.41	1.16	1.29		+101.22 \pm 0.34
S6	−49.34	−48.84	−49.13	−47.35	−47.34		0.98	0.74	0.21	1.70	0.86		−49.01 \pm 0.19

^aResults were not considered for calculation of weighted mean values as the applied technique is associated with a higher uncertainty.

uncertainty (σ) of individual laboratory results was estimated using the law of error propagation including the uncertainty in the international standards, their analyses, and the analyses of the NH_4NO_3 samples (Equations 1 and 2).

For $\delta^{15}\text{N}(\text{NH}_4\text{NO}_3)$, all results obtained by EA/IRMS were included for calculation of the weighted mean value except for results by one laboratory (Lab 4), as this laboratory used a more complicated analytical procedure with higher uncertainties. For $\delta^{15}\text{N}(\text{NO}_3^-)$ and $\delta^{15}\text{N}(\text{NH}_4^+)$, all laboratory results were included to calculate the weighted mean values, irrespective of the applied analytical technique.

A comparison of $\delta^{15}\text{N}(\text{NH}_4\text{NO}_3)$ with average $\delta^{15}\text{N}(\text{NH}_4^+)/\delta^{15}\text{N}(\text{NO}_3^-)$ values indicates a good agreement to within <0.2‰. Nonetheless, results by individual laboratories for moiety-specific δ values deviate substantially from the weighted mean. As an example, $\delta^{15}\text{N}(\text{NO}_3^-)$ results from Lab 8 are substantially higher than those from other laboratories by an average of (+2.15 \pm 0.58)‰. This may be due to the specific preparation technique applied, NH_4^+ removal by ion exchange, a technique which is prone to preferential retention/elution of $^{15}\text{NO}_3^-$.⁵² In contrast, microdiffusion methods tend to underestimate $\delta^{15}\text{N}$ values of both NO_3^- and NH_4^+ , which may be

reflected in the $\delta^{15}\text{N}(\text{NH}_4^+)$ values of Lab 6 but not those of Lab 5, where a similar technique was used. Conversely, systematic fractionation effects by preparation techniques should be accounted for by identical treatment (IT) of the provided IAEA and USGS standards used for data correction. In summary, analysis of $\delta^{15}\text{N}(\text{NH}_4^+)$ and $\delta^{15}\text{N}(\text{NO}_3^-)$ is still challenging; however, the ensemble of techniques applied in this study provides good agreement with $\delta^{15}\text{N}(\text{NH}_4\text{NO}_3)$ values.

3.1.2 | Optimal reaction conditions for NH_4NO_3 thermal decomposition to N_2O

Under optimised reaction conditions (270°C, 24 h) and distillation procedure, an average N_2O yield of 93–95% was achieved for the decomposition of NH_4NO_3 salts S1–S6 (Table S1, supporting information). The yield and repeatability of the decomposition reaction are somewhat better than reported in our earlier study (91.2–93.5%)²⁵ and published by Toyoda et al.¹ (90.1 \pm 3.7)%, $n = 3$), surpasses results by Westley et al.²³ (65.6 \pm 5.1)%, $n = 20$). A further increase in the yield of the NH_4NO_3 decomposition was achieved by

conducting the reaction in a NH_4HSO_4 – $(\text{NH}_4)_2\text{SO}_4$ melt (around 2%), as suggested for industrial applications by Szabó et al.⁴³ This variant displayed comparable $\delta^{15}\text{N}^\alpha$ values but a loss in the $\delta^{15}\text{N}^\beta$ information due to NH_4^+ salt addition, and was thus not continued.

No correction was applied to $\delta^{15}\text{N}^\alpha$ and $\delta^{15}\text{N}^\beta$ for the loss in N_2O (around 5–7%), mainly due to uncertainties in the reaction mechanisms (incomplete decomposition or side-reaction), which makes it difficult to estimate the effect on δ values. Assuming incomplete reaction accompanied by fractionation effects, according to our earlier study,²⁵ a 5% reduction in yield for S1–S6 should result in 0.7/3.0/1.8‰ lower $\delta^{15}\text{N}^\alpha/\delta^{15}\text{N}^\beta/\delta^{15}\text{N}^\text{SP}$ values, respectively. However, a much smaller difference in $\delta^{15}\text{N}$ was observed when comparing results of N_2O RMs analysed by QCLAS (calibrated by NH_4NO_3 decomposition) with IRMS analyses. Therefore, our assumption is that the decrease in yield is at least partly caused by a “branching” side reaction, e.g. nitrogen gas (N_2) production,⁵³ which was observed to display higher $\delta^{15}\text{N}(\text{N}_2)$ values.¹ We speculate that N_2 production has a minor effect on $\delta^{15}\text{N}^\alpha$, $\delta^{15}\text{N}^\beta$ and $\delta^{15}\text{N}^\text{SP}$, but the effect is expected to depend on the timing of N_2 generation, which is not known.

3.1.3 | Consistency of isotopic composition of S1– N_2O –S6– N_2O

A general goal of the current project was to provide a link to the Air– N_2 scale and to determine the N_2O site-specific isotopic composition across a wide range of δ values. Therefore, the consistency of the isotopic composition of the N_2O gases ($\delta^{15}\text{N}^\beta$ and $\delta^{15}\text{N}^\alpha$, S1– N_2O –S6– N_2O) and the NH_4NO_3 salts ($\delta^{15}\text{N}(\text{NH}_4^+)$ and $\delta^{15}\text{N}(\text{NO}_3^-)$, S1–S6) was tested. The detailed procedure is described in section 2.1.3. In short, assuming the validity of the NH_4NO_3 decomposition reaction,

measured $\delta^{15}\text{N}^\alpha$ values of S1– N_2O /S4– N_2O and actual $\delta^{15}\text{N}^\alpha$ values, i.e. $\delta^{15}\text{N}(\text{NO}_3^-)$ of the educt NH_4NO_3 salts S1/S4, were used to define a linear calibration function. $\delta^{15}\text{N}^\alpha_{\text{cal}}$ values of S2– N_2O , S3– N_2O , S5– N_2O and S6– N_2O were calculated from measured $\delta^{15}\text{N}^\alpha$ using this correction function and compared against actual values (Table 6).

Results of $\delta^{15}\text{N}^\alpha_{\text{cal}}/\delta^{15}\text{N}^\beta_{\text{cal}}/\delta^{15}\text{N}^\text{SP}_{\text{cal}}$ for S2– N_2O and S3– N_2O agree within expanded uncertainties ($2 \times \sigma_{\text{cal}}$, Equation 2) with the isotopic composition of the substrate NH_4NO_3 (S2, S3; Table 5). In contrast, for S5– N_2O and S6– N_2O , $\delta^{15}\text{N}^\alpha_{\text{cal}}/\delta^{15}\text{N}^\beta_{\text{cal}}/\delta^{15}\text{N}^\text{SP}_{\text{cal}}$ values of the N_2O gases show a significant deviation from $\delta^{15}\text{N}(\text{NO}_3^-)/\delta^{15}\text{N}(\text{NH}_4^+)/\delta^{15}\text{N}(\text{NO}_3^-) - \delta^{15}\text{N}(\text{NH}_4^+)$ of the respective salts (S5, S6). Assuming similar fractionation effects for decomposition of all NH_4NO_3 salts (S1–S6), provided the comparable decomposition yield (Table S1, supporting information), we conclude that the deviation is caused by non-linearities either in N_2O isotope analysis by QCLAS or in $\delta^{15}\text{N}(\text{NO}_3^-)$ and $\delta^{15}\text{N}(\text{NH}_4^+)$ analyses of the NH_4NO_3 salts. The latter is more plausible, as the QCLAS analyses using the same calibration approach showed good agreement with independent IRMS measurements for N_2O RM with high ^{15}N enrichment (see RM4, Table S2, supporting information). The observed deviations were highest for $\delta^{15}\text{N}^\beta_{\text{cal}}$ to $\delta^{15}\text{N}(\text{NH}_4^+)$ (e.g. S5), which agrees with earlier studies indicating challenges in $\delta^{15}\text{N}(\text{NH}_4^+)$ analysis, but this may also be due to the lack of available international standards for $\delta^{15}\text{N}(\text{NH}_4^+)$ that cover δ values above $(+53.75 \pm 0.24)\text{‰}$ (USGS26) and below $(-30.41 \pm 0.27)\text{‰}$ (USGS25).

In summary, our results demonstrate consistency of the isotopic composition of the N_2O gases from around zero (S1– N_2O) to ^{15}N -enriched (S4– N_2O) and of the substrate NH_4NO_3 salts (S1–S4). Thereby, our study covers a much larger range of δ values ($> 50\text{‰}$ in $\delta^{15}\text{N}^\alpha_{\text{cal}}$ and $\delta^{15}\text{N}^\beta_{\text{cal}}$) than earlier studies,^{1,23} and provides a robust link to the Air– N_2 scale. At very high and low ^{15}N enrichment

TABLE 6 Consistency check for $\delta^{15}\text{N}^\alpha_{\text{cal}}$, $\delta^{15}\text{N}^\beta_{\text{cal}}$, $\delta^{15}\text{N}^\text{SP}_{\text{cal}}$ and $\delta^{15}\text{N}_{\text{cal}}$ of N_2O gases (S2– N_2O , S3– N_2O , S5– N_2O , S6– N_2O) as analysed by QCLAS and referenced to the actual isotopic composition of S1– N_2O and S4– N_2O ; against the actual isotopic composition of the same gases, expressed by $\delta^{15}\text{N}(\text{NO}_3^-)$, $\delta^{15}\text{N}(\text{NH}_4^+)$, $\delta^{15}\text{N}(\text{NO}_3^-) - \delta^{15}\text{N}(\text{NH}_4^+)$ and $\delta^{15}\text{N}(\text{NH}_4\text{NO}_3)$ of the respective NH_4NO_3 substrates (S2, S3, S5, S6). For details see section 2.1.3. The number of repetitions (n) for S2– N_2O /S3– N_2O analysis is 3, for S5– N_2O and S6– N_2O it is 10. All values are reported in ‰

	Isotopic composition of N ₂ O as analysed by QCLAS (Sx-N ₂ O)							
	$\delta^{15}\text{N}^{\alpha}_{\text{cal}}$	σ	$\delta^{15}\text{N}^{\beta}_{\text{cal}}$	σ	$\delta^{15}\text{N}^{\text{SP}}_{\text{cal}}$	σ	$\delta^{15}\text{N}_{\text{cal}}$	σ
S2-N ₂ O	+13.20	0.23	+13.99	0.29	−0.79	0.37	+13.60	0.37
S3-N ₂ O	+13.70	0.17	+0.36	0.24	+13.34	0.30	+7.03	0.30
S5-N ₂ O	+113.53	0.24	+103.67	0.32	+9.78	0.41	+108.60	0.41
S6-N ₂ O	−51.26	0.17	−50.03	0.24	−1.27	0.30	−50.60	0.30
	Actual isotopic composition derived from NH ₄ NO ₃ (Sx)							
	$\delta^{15}\text{N}(\text{NO}_3^-)$	σ	$\delta^{15}\text{N}(\text{NH}_4^+)$	σ	$\delta^{15}\text{N}(\text{NO}_3^-) - \delta^{15}\text{N}(\text{NH}_4^+)$	σ	$\delta^{15}\text{N}(\text{NH}_4\text{NO}_3)$	σ
S2	+13.69	0.07	+14.26	0.13	−0.57	0.15	+14.14	0.08
S3	+14.04	0.09	+0.19	0.08	+13.85	0.12	+7.31	0.06
S5	+114.37	0.15	+101.22	0.34	+13.16	0.37	+107.90	0.13
S6	−50.47	0.08	−49.01	0.19	−1.46	0.21	−49.87	0.09

(S5-N₂O, S6-N₂O), the calibration approach using NH₄NO₃ decomposition is more challenging, probably due to less satisfying analytical accuracy of $\delta^{15}\text{N}(\text{NH}_4^+)$ measurements to date. As the N₂O gases S5-N₂O and S6-N₂O were not included in the analysis of N₂O RMs, their enhanced uncertainty in $\delta^{15}\text{N}^{\alpha}_{\text{cal}}$ and $\delta^{15}\text{N}^{\beta}_{\text{cal}}$ does not affect the data quality of N₂O RMs.

3.2 | Isotopic composition of N₂O RMs

3.2.1 | Isotopic composition of N₂O RMs for $\delta^{15}\text{N}^{\text{SP}}$ by QCLAS and IRMS

The novel N₂O RMs (RM1–RM5) were calibrated against Air-N₂ by both QCLAS (Lab Empa) and IRMS (Lab TT) analyses. For QCLAS analyses, two N₂O gases produced by NH₄NO₃ decomposition (S1-N₂O, S4-N₂O) were applied to define a calibration function and propagate the isotopic information of the NH₄NO₃ salts ($\delta^{15}\text{N}(\text{NO}_3^-)$, $\delta^{15}\text{N}(\text{NH}_4^+)$) to the N₂O RMs ($\delta^{15}\text{N}^{\alpha}$, $\delta^{15}\text{N}^{\beta}$). $\delta^{15}\text{N}^{\text{SP}}$ and $\delta^{15}\text{N}$ were calculated using definitions and their uncertainty estimated using the law of error propagation. In Table 7, $\delta^{15}\text{N}^{\text{SP}}$ values acquired by QCLAS (Lab Empa) using the calibration approach established in this study are compared with results provided by DI-IRMS (Lab TT) using a

previously published link to the Air-N₂ scale.¹ The complete QCLAS and DI-IRMS datasets for N₂O RMs are shown in Tables S2 and S3 (supporting information).

Results in Table 7 indicate a 1.5–2.7‰ offset in $\delta^{15}\text{N}^{\text{SP}}$ measurements by DI-IRMS (Lab TT, Tokyo Institute of Technology) and QCLAS (Lab Empa) across all N₂O RMs. This is most likely attributable to the calibration of the position-dependent δ values with respect to Air-N₂ via the NH₄NO₃ decomposition technique, which were performed independently for the two labs. Incidentally, for the NH₄NO₃ salts S1–S4, the $\delta^{15}\text{N}(\text{NO}_3^-)$ results provided by Lab TT were always lower (-0.63 ± 0.59 ‰), while $\delta^{15}\text{N}(\text{NH}_4^+)$ values were higher than the respective weighted mean values ($+0.49 \pm 0.25$ ‰), which would lead to 1.12‰ lower $\delta^{15}\text{N}^{\text{SP}}$ values (Table 5).

A similar 1.5–2.0‰ difference in $\delta^{15}\text{N}^{\text{SP}}$ results was recently detected by Kantnerová et al.⁵⁴ using an independent approach, equilibrating N₂O at 200°C over a catalyst and comparing theoretical predictions with analytical results traceable to the $\delta^{15}\text{N}^{\text{SP}}$ scale of Lab TT. One previous comparison using an independent link to the Air-N₂ scale also indicated 1.5‰ higher $\delta^{15}\text{N}^{\text{SP}}$ values: $(+20.2 \pm 2.1)$ ‰ vs. $(+18.7 \pm 2.2)$ ‰ for ambient tropospheric N₂O.²⁴ Other studies confirmed the $\delta^{15}\text{N}^{\text{SP}}$ measurements by the Tokyo Institute of Technology, using the NH₄NO₃ decomposition technique.^{23,25} The uncertainty of both approaches, however, was quite high.

TABLE 7 $\delta^{15}\text{N}^{\text{SP}}$ analyses of N₂O RMs by QCLAS (Lab Empa) referenced to Air-N₂ by NH₄NO₃ decomposition as performed in this study (S1-N₂O/S4-N₂O) and by DI-IRMS¹ (Lab TT). All values are reported in ‰

	Lab Empa (QCLAS)		Lab TT (DI-IRMS)		Difference $\delta^{15}\text{N}^{\text{SP}}$ (Lab Empa – Lab TT)	
	$\delta^{15}\text{N}^{\text{SP}}$	σ	$\delta^{15}\text{N}^{\text{SP}}$	σ		σ
RM1A	+0.47	0.26	−1.04	0.91	+1.51	0.95
RM1B	+0.30	0.30	−1.19	0.91	+1.49	0.96
RM2	+18.92	0.24	+17.00	0.91	+1.92	0.94
RM3A	−2.13	0.37	−4.13	0.93	+2.00	1.00
RM3B	+1.01	0.23	−0.68	0.91	+1.69	0.94
RM4	+0.00	0.60	−2.75	0.93	+2.75	1.11
RM5	+21.96	0.33	+20.20	0.91	+1.76	0.97

TABLE 8 $\delta^{15}\text{N}$ analyses of N₂O RMs by IRMS at the Tokyo Institute of Technology (Lab TT: Thermo MAT252), MPI-BGC (Lab MPI-I: Thermo Delta Plus, Lab MPI-II: Thermo MAT 253), and UEA (Lab UEA-I: Sercon GEO 20-20, Lab UEA-II: Finnigan MAT 253) using independent calibration approaches. The ¹⁷O correction of DI-IRMS was conducted using actual $\Delta^{17}\text{O}$ values. All values are reported in ‰. The full set of analyses for all laboratories is provided in Table 9 (Lab MPI-II) and in the supporting information (Lab TT: Table S3, Lab MPI-I: Table S4, Lab UEA-I: Table S5, Lab UEA-II: Table S6)

	Lab TT	Lab MPI-I	Lab MPI-II	Lab UEA-I	Lab UEA-II	σ TT	σ MPI-I	σ MPI-II	σ UEA-I	σ UEA-II	Weighted mean $\pm \sigma$
RM1A	+0.67	+0.44	+0.29	+0.29	+0.28	0.45	0.16	0.21	0.13	0.06	+0.30 \pm 0.05
RM1B	+0.53	+0.33	+0.20	+0.24	+0.19	0.45	0.14	0.21	0.10	0.06	+0.22 \pm 0.05
RM2	+7.31	+7.09	+6.95	+6.73	+6.94	0.45	0.16	0.21	0.07	0.06	+6.88 \pm 0.04
RM3A	+53.41	+53.25	+53.11	+52.69	+53.09	0.47	0.15	0.21	0.11	0.07	+53.02 \pm 0.05
RM3B	+16.45	+16.14	+16.09	+15.96	+16.08	0.46	0.14	0.21	0.17	0.06	+16.08 \pm 0.05
RM4	+104.54	+104.39	+104.33	+104.18	+104.30	0.50	0.37	0.28	0.13	0.08	+104.28 \pm 0.06
RM5	+33.76	+33.52	+33.46	+33.38	+33.45	0.46	0.21	0.21	0.10	0.06	+33.44 \pm 0.05

We conclude that the realisation of the link between $\delta^{15}\text{N}^{\text{SP}}$ and the Air- N_2 scale with high accuracy is still challenging and the current realisation of the Air- N_2 scale for $\delta^{15}\text{N}^{\text{SP}}$ provided by USGS51 and USGS52²⁶ may lead to too low $\delta^{15}\text{N}^{\text{SP}}$ values and should be revisited in future studies.

3.2.2 | Isotopic composition of N_2O RMs for $\delta^{15}\text{N}$ by IRMS

$\delta^{15}\text{N}$ values of N_2O RMs were analysed by IRMS in three different laboratories using independent links to the Air- N_2 scale (Table 8). Results display a consistent offset of $(+0.22 \pm 0.05)\text{‰}$ and $(+0.46 \pm 0.14)\text{‰}$ between Lab MPI-I (EA/IRMS, Thermo Delta Plus, MPI-

BGC) and Lab UEA-I (Sercon GEO 20-20, UEA) versus Lab TT (Thermo MAT252, Tokyo Institute of Technology). A slightly larger offset was detected for the N_2O RMs USGS51 and USGS52 (Table 9) by a comparison of published provisional values (Lab TT)²⁶ and results of MPI-II, with $\delta^{15}\text{N}$ values of $(+0.92 \pm 0.22)\text{‰}$ (USGS51) and $(+0.07 \pm 0.22)\text{‰}$ (USGS52). These values fall between results published by laboratories 7 and 8 (USGS and BGC-IsoLab) in Ostrom et al,²⁶ and are lower than results of the other laboratories, highlighting an ongoing scaling problem in $\delta^{15}\text{N}(\text{N}_2\text{O})$ measurements. A similar offset between laboratories had already been detected earlier and was attributed to differences in the propagation of the Air- N_2 scale to $\delta^{15}\text{N}(\text{N}_2\text{O})$.^{20,25,26} To account for differences between individual approaches to anchor laboratory results to scales, a weighted mean value was calculated for N_2O RMs.

TABLE 9 DI-IRMS analyses of RMs, USGS51, USGS52 and NINO at MPI-BGC (MPI-II). Analyses were conducted in two campaigns in September 2019 and February 2021 on individual sample flasks. For RM1A, in each campaign three flask samples were analysed; for RM2, two flask samples were analysed in 2021. Referencing and ^{17}O corrections considered actual $\Delta^{17}\text{O}$ values: δ values were referenced to Air- N_2 and VSMOW using the in-house working standard NINO ($\delta^{15}\text{N}$) and USGS51 ($\delta^{18}\text{O}$) and calculated according to Kaiser et al.⁴⁷ n indicates the number of repeated analyses per campaign. Uncertainties for individual campaigns are calculated following the law of error propagation. For the uncertainty of the weighted mean, the uncertainty of the working standard was applied, which was considered as a conservative approach. All values are reported in ‰

	Sep 2019					Feb 2021					Weighted mean $\pm \sigma$	
	$\delta^{15}\text{N}$	σ	$\delta^{18}\text{O}$	σ	n	$\delta^{15}\text{N}$	σ	$\delta^{18}\text{O}$	σ	n	$\delta^{15}\text{N}$	$\delta^{18}\text{O}$
RM1A	+0.30	0.22	+39.51	0.35	9	+0.29	0.23	+39.48	0.38	9	+0.29 \pm 0.21	+39.50 \pm 0.34
RM1B	+0.20	0.23	+39.14	0.36	3	+0.19	0.24	+39.10	0.38	3	+0.20 \pm 0.21	+39.12 \pm 0.34
RM2	+6.96	0.23	+44.37	0.35	3	+6.94	0.24	+44.32	0.38	6	+6.95 \pm 0.21	+44.35 \pm 0.34
RM3A	+53.12	0.25	+103.60	0.37	3	+53.09	0.26	+103.50	0.41	3	+53.11 \pm 0.21	+103.55 \pm 0.34
RM3B	+16.10	0.23	+55.58	0.35	3	+16.08	0.24	+55.55	0.39	3	+16.09 \pm 0.21	+55.57 \pm 0.34
RM4	+104.33	0.28	+154.93	0.38	3	n.a.	n.a.	n.a.	n.a.	n.a.	+104.33 \pm 0.21	+154.93 \pm 0.38
RM5	+33.48	0.23	+39.77	0.35	3	+33.44	0.25	+39.74	0.38	3	+33.46 \pm 0.21	+39.76 \pm 0.34
USGS51	+0.92	0.22	+41.45 ^a	0.35 ^a	6	n.a.	n.a.	n.a.	n.a.	n.a.	+0.92 \pm 0.22	+41.45 \pm 0.35 ^a
USGS52	+0.07	0.22	+40.89	0.35	6	n.a.	n.a.	n.a.	n.a.	n.a.	+0.07 \pm 0.22	+40.89 \pm 0.35
NINO	+0.54 ^b	0.22 ^b	+39.90	0.35	6	+0.53 ^c	0.23 ^c	+39.90 ^c	0.38 ^c	9	+0.54 \pm 0.21 ^b	+39.90 \pm 0.34

n.a. not analysed.

^aAverage of laboratory results from Ostrom et al²⁶ taken for referencing of $\delta^{18}\text{O}$

^bValue provided by EA/IRMS analysis (Table S4, supporting information), value taken for referencing of $\delta^{15}\text{N}$

^cAnalysed as quality control.

TABLE 10 $\delta^{18}\text{O}$ analyses of N_2O RMs by IRMS at the Tokyo Institute of Technology (Lab TT: Thermo MAT252), MPI-BGC (Lab MPI-II: Thermo MAT 253), and UEA (Lab UEA-I: Sercon GEO 20-20, Lab UEA-II: Finnigan MAT 253). All values are reported in ‰. The full set of analyses for all laboratories is provided in the supporting information (Lab TT: Table S3, Lab UEA-I: Table S5)

	Lab TT	Lab MPI-II	Lab UEA-I	Lab UEA-II	σ TT	σ MPI-II	σ UEA-I	σ UEA-II	Weighted mean $\pm \sigma$
RM1A	+39.37	+39.50	+39.06	+39.22	1.24	0.34	0.25	0.22	+39.22 \pm 0.15
RM1B	+38.86	+39.12	+38.77	+38.83	1.24	0.34	0.24	0.22	+38.86 \pm 0.15
RM2	+44.08	+44.35	+43.69	+44.02	1.25	0.34	0.24	0.22	+43.96 \pm 0.15
RM3A	+103.21	+103.55	+103.04	+102.78	1.30	0.34	0.27	0.24	+103.04 \pm 0.16
RM3B	+55.28	+55.57	+54.98	+55.13	1.26	0.34	0.26	0.22	+55.17 \pm 0.15
RM4	+154.35	+154.93	+155.17	+153.63	1.36	0.38	0.39	0.24	+154.25 \pm 0.18
RM5	+39.50	+39.76	+39.43	+39.50	1.29	0.34	0.24	0.22	+39.52 \pm 0.15

In contrast, differences between analytical techniques applied within one lab, thus using the same link to the scale, were smaller than offsets between laboratories: $(+0.10 \pm 0.04)\text{‰}$ for Lab MPI and $(+0.12 \pm 0.14)\text{‰}$ for Lab UEA. This indicates that both EA/IRMS and GC-IRMS and DI-IRMS can achieve high accuracy, provided that an accurate link to the scale and $\Delta^{17}\text{O}$ data are available. Consistency of N_2O RM flask subsamples was demonstrated using DI-IRMS (Lab MPI-II, Table 9) by replicate sampling and analysis in two campaigns in September 2019 and February 2021. For RM1A, a total of six independent flask samples were analysed; the results agreed to within 0.02‰ for $\delta^{15}\text{N}(\text{N}_2\text{O})$ and 0.03‰ for $\delta^{18}\text{O}(\text{N}_2\text{O})$ (2σ , data not shown).

3.2.3 | Isotopic composition of N_2O RMs for $\delta^{18}\text{O}$ and $\delta^{17}\text{O}$ by IRMS

$\delta^{18}\text{O}$ values of N_2O RMs were analysed by IRMS in three different laboratories (Table 10). Results show deviations of $(+0.30 \pm 0.13)\text{‰}$, $(+0.22 \pm 0.24)\text{‰}$ and $(+0.07 \pm 0.38)\text{‰}$ between Lab TT and Lab MPI-II, Lab UEA-I and Lab UEA-II, respectively. Differences were highest for N_2O RMs with high $\delta^{18}\text{O}$ values (RM3A, RM4), indicating a potential scaling or scale compression issue. Measurements were not completely independent for all laboratories, as the results for Lab MPI-II were referenced to average $\delta^{18}\text{O}$ values of USGS51 in Ostrom et al.,²⁶ which in turn was determined by seven laboratories.

$\delta^{17}\text{O}$ values were determined by GC/IRMS at UEA (Lab UEA-I) and showed a $(0.98 \pm 0.27)\text{‰}$ offset to prototypical measurements by HR-IRMS (MAT253 ULTRA) at the Tokyo Institute of Technology (Lab

TT; Table 11). Consistency of GC/IRMS results agreed with an approximation, where the $\delta^{17}\text{O}$ was calculated from the ^{17}O content of the ^{18}O -labelled H_2O used for ^{18}O -labelled NH_4NO_3 and N_2O production (certificate of analysis provided by Medical Isotopes Inc., USA; see Supplementary Method 2, supporting information). A 1‰ error in $\delta^{17}\text{O}$ results in around -0.1‰ error in $\delta^{15}\text{N}^{\text{q}}$, when used for correction of DI-IRMS measurements.

4 | CONCLUSIONS

Within the SIRS project, we established seven pure N_2O isotope RMs, which were analysed by specialised laboratories against the international isotope-ratio scales. The established N_2O isotope RMs offer a wide coverage of δ values (Table 12) beyond the currently available standards USGS51 and USGS52. This will enable future users to implement the recommended two-point calibration approach for IRMS instrumentation, and, upon dilution with an appropriate gas matrix, for laser spectroscopic techniques as well.^{19,55} In addition, the gases have been characterised for their $\delta^{17}\text{O}$ signatures in order to improve data quality/correction algorithms with respect to $\delta^{15}\text{N}^{\text{SP}}$ and $\delta^{15}\text{N}$ analysis by mass spectrometry. In summary, the novel N_2O isotope RMs are expected to improve compatibility between laboratories and accelerate the progress in this emerging field of research.

ACKNOWLEDGMENTS

This project, 16ENV06 Metrology for Stable Isotope Reference Standards (SIRS), received funding from the EMPIR program co-financed by the Participating States and from the European Union's Horizon 2020 research and innovation program. Longfei Yu was supported by the Swiss National Science Foundation (SNSF; grant number 200021_163075), as well as the EMPAPOSTDOCS-II program, which received funding from the European Union's H2020 Marie Skłodowska-Curie Actions (EMPAPOSTDOCS-II; grant number 754364). Kristýna Kantnerová was supported by the SNSF (grant number 200021_166255) and the bilateral Japanese Swiss Science and Technology Program (JSPS International Fellowship for Research in Japan; grant number GR18108). The authors would like to thank Daniel Zindel from ETH Zurich for providing laboratory equipment and space for the synthesis of the ^{18}O -labelled NH_4NO_3 . Open Access Funding provided by ETH-Bereich Forschungsanstalten.

TABLE 11 $\delta^{17}\text{O}$ analyses of N_2O RMs by GC/IRMS at UEA (Lab UEA-I), HR-IRMS at the Tokyo Institute of Technology (Lab TT), and predictions based on mixing of ^{18}O -labelled N_2O with commercial N_2O . All values are reported in ‰

	Lab TT	Lab UEA-I	Predicted	σ TT	σ UEA-I
RM1A	+21.60	+20.33	+20.4	0.08	0.59
RM1B		+20.88	+20.2		0.56
RM2		+20.87	+20.8		0.40
RM3A	+24.40	+23.78	+24.5	0.21	0.54
RM3B		+21.22	+21.5		0.24
RM4	+27.75	+26.71	+27.6	0.35	0.83
RM5		+20.90	+20.6		0.44

TABLE 12 Weighted mean δ values for the N_2O RMs. All values are reported in ‰

	$\delta^{15}\text{N}^{\text{SP}}$	σ	$\delta^{15}\text{N}$	σ	$\delta^{18}\text{O}$	σ	$\delta^{17}\text{O}$	σ
RM1A	-1.04	0.91	+0.30	0.05	+39.22	0.15	+20.33	0.59
RM1B	-1.19	0.91	+0.22	0.05	+38.86	0.15	+20.88	0.56
RM2	+17.00	0.91	+6.88	0.04	+43.96	0.15	+20.87	0.40
RM3A	-4.13	0.93	+53.02	0.05	+103.04	0.16	+23.78	0.54
RM3B	-0.68	0.91	+16.08	0.05	+55.17	0.15	+21.22	0.24
RM4	-2.75	0.93	+104.28	0.06	+154.25	0.18	+26.71	0.83
RM5	+20.20	0.91	+33.44	0.05	+39.52	0.15	+20.90	0.44














PEER REVIEW

The peer review history for this article is available at <https://publons.com/publon/10.1002/rcm.9296>.

DATA AVAILABILITY STATEMENT

The data that supports the findings of this study are available in the supplementary material of this article. Further data are available from the corresponding author upon reasonable request.

ORCID

Joachim Mohn  <https://orcid.org/0000-0002-9799-1001>
 Christina Biasi  <https://orcid.org/0000-0002-7413-3354>
 Samuel Bodé  <https://orcid.org/0000-0002-0258-6450>
 Pascal Boeckx  <https://orcid.org/0000-0003-3998-0010>
 Sarah Eggleston  <https://orcid.org/0000-0003-2775-8826>
 Myriam Guillevic  <https://orcid.org/0000-0002-8128-7247>
 Jan Kaiser  <https://orcid.org/0000-0002-1553-4043>
 Heiko Moossen  <https://orcid.org/0000-0003-4768-2603>
 Mayuko Nakagawa  <https://orcid.org/0000-0003-3611-8118>
 Sakae Toyoda  <https://orcid.org/0000-0003-1624-5910>
 Wolfgang Wanek  <https://orcid.org/0000-0003-2178-8258>
 Naohiro Yoshida  <https://orcid.org/0000-0003-0454-3849>
 Longfei Yu  <https://orcid.org/0000-0002-2127-6343>

REFERENCES

- Toyoda S, Yoshida N. Determination of nitrogen isotopomers of nitrous oxide on a modified isotope ratio mass spectrometer. *Anal Chem*. 1999;71(20):4711-4718. doi:10.1021/ac9904563
- Toyoda S, Yoshida N, Koba K. Isotopocule analysis of biologically produced nitrous oxide in various environments. *Mass Spectrom Rev*. 2017;36(2):135-160. doi:10.1002/mas.21459
- Ostrom NE, Ostrom PH. Mining the isotopic complexity of nitrous oxide: A review of challenges and opportunities. *Biogeochemistry*. 2017;132(3):359-372. doi:10.1007/s10533-017-0301-5
- Decock C, Six J. How reliable is the intramolecular distribution of ^{15}N in N_2O to source partition N_2O emitted from soil? *Soil Biol Biochem*. 2013;65:114-127. doi:10.1016/j.soilbio.2013.05.012
- Denk TRA, Mohn J, Decock C, et al. The nitrogen cycle: A review of isotope effects and isotope modeling approaches. *Soil Biol Biochem*. 2017;105:121-137. doi:10.1016/j.soilbio.2016.11.015
- Yu L, Harris E, Lewicka-Szczepak D, et al. What can we learn from N_2O isotope data? - Analytics, processes and modelling. *Rapid Commun Mass Spectrom*. 2020;34(20):e8858. doi:10.1002/rcm.8858
- Koba K, Osaka K, Tobari Y, et al. Biogeochemistry of nitrous oxide in groundwater in a forested ecosystem elucidated by nitrous oxide isotopomer measurements. *Geochim Cosmochim Acta*. 2009;73(11):3115-3133. doi:10.1016/j.gca.2009.03.022
- Lewicka-Szczepak D, Augustin J, Giesemann A, Well R. Quantifying N_2O reduction to N_2 based on N_2O isotopocules-validation with independent methods (helium incubation and ^{15}N gas flux method). *Biogeosciences*. 2017;14(3):711-732. doi:10.5194/bg-14-711-2017
- Denk TRA, Kraus D, Kiese R, Butterbach-Bahl K, Wolf B. Constraining N cycling in the ecosystem model LandscapeDNDC with the stable isotope model SIMONE. *Ecology*. 2019;100(5):e02675. doi:10.1002/ecy.2675
- Ibraim E, Denk T, Wolf B, et al. Denitrification is the main nitrous oxide source process in grassland soils according to quasi-continuous isotopocule analysis and biogeochemical modeling. *Global Biogeochem Cycles*. 2020;34(6). doi:10.1029/2019GB006505
- Bourbonnais A, Letscher RT, Bange HW, et al. N_2O production and consumption from stable isotopic and concentration data in the Peruvian coastal upwelling system. *Global Biogeochem Cycles*. 2017;31(4):678-698. doi:10.1002/2016GB005567
- Bai E, Houlton BZ, Wang YP. Isotopic identification of nitrogen hotspots across natural terrestrial ecosystems. *Biogeosciences*. 2012;9(8):3287-3304. doi:10.5194/bg-9-3287-2012
- Brenninkmeijer CAM, Röckmann T. Mass spectrometry of the intramolecular nitrogen isotope distribution of environmental nitrous oxide using fragment-ion analysis. *Rapid Commun Mass Spectrom*. 1999;13(20):2028-2033.
- Wächter H, Mohn J, Tuzson B, Emmenegger L, Sigrist MW. Determination of N_2O isotopomers with quantum cascade laser based absorption spectroscopy. *Opt Express*. 2008;16(12):9239-9244. doi:10.1364/OE.16.009239
- Mohn J, Tuzson B, Manninen A, et al. Site selective real-time measurements of atmospheric N_2O isotopomers by laser spectroscopy. *Atmos Meas Tech*. 2012;5(7):1601-1609. doi:10.5194/amt-5-1601-2012
- Erlor DV, Duncan TM, Murray R, et al. Applying cavity ring-down spectroscopy for the measurement of dissolved nitrous oxide concentrations and bulk nitrogen isotopic composition in aquatic systems: Correcting for interferences and field application. *Limnol Oceanogr - Meth*. 2015;13(8):391-401. doi:10.1002/lom3.10032
- Winther M, Balslev-Harder D, Christensen S, et al. Continuous measurements of nitrous oxide isotopomers during incubation experiments. *Biogeosciences*. 2018;15(3):767-780. doi:10.5194/bg-15-767-2018
- Haslun JA, Ostrom NE, Hegg EL, Ostrom PH. Estimation of isotope variation of N_2O during denitrification by *Pseudomonas aureofaciens* and *Pseudomonas chlororaphis*: Implications for N_2O source apportionment. *Biogeosciences*. 2018;15(12):3873-3882. doi:10.5194/bg-15-3873-2018
- Harris SJ, Lissberg J, Xia L, et al. N_2O isotopocule measurements using laser spectroscopy: Analyzer characterization and intercomparison. *Atmos Meas Tech*. 2020;13(5):2797-2831. doi:10.5194/amt-13-2797-2020
- Mohn J, Wolf B, Toyoda S, et al. Interlaboratory assessment of nitrous oxide isotopomer analysis by isotope ratio mass spectrometry and laser spectroscopy: Current status and perspectives. *Rapid Commun Mass Spectrom*. 2014;28(18):1995-2007. doi:10.1002/rcm.6982
- Brewer PJ, Kim JS, Lee S, et al. Advances in reference materials and measurement techniques for greenhouse gas atmospheric observations. *Metrologia*. 2019;56(3):034006. doi:10.1088/1681-7575/ab1506
- Friedman L, Bigeleisen J. Oxygen and nitrogen isotope effects in the decomposition of ammonium nitrate. *J Chem Phys*. 1950;18(10):1325-1331. doi:10.1063/1.1747471
- Westley MB, Popp BN, Rust TM. The calibration of the intramolecular nitrogen isotope distribution in nitrous oxide measured by isotope ratio mass spectrometry. *Rapid Commun Mass Spectrom*. 2007;21(3):391-405. doi:10.1002/rcm.2828
- Griffith DWT, Parkes SD, Haverd V, Paton-Walsh C, Wilson SR. Absolute calibration of the intramolecular site preference of ^{15}N fractionation in tropospheric N_2O by FT-IR spectroscopy. *Anal Chem*. 2009;81(6):2227-2234. doi:10.1021/ac802371c
- Mohn J, Gutjahr W, Toyoda S, et al. Reassessment of the NH_4NO_3 thermal decomposition technique for calibration of the N_2O isotopic composition. *Rapid Commun Mass Spectrom*. 2016;30(23):2487-2496. doi:10.1002/rcm.7736
- Ostrom NE, Gandhi H, Coplen TB, et al. Preliminary assessment of stable nitrogen and oxygen isotopic composition of USGS51 and USGS52 nitrous oxide reference gases and perspectives on

- calibration needs. *Rapid Commun Mass Spectrom.* 2018;32(15):1207-1214. doi:[10.1002/rcm.8157](https://doi.org/10.1002/rcm.8157)
27. Ostrom NE, Gandhi H, Coplen TB, et al. Erratum to: Preliminary assessment of stable nitrogen and oxygen isotopic composition of USGS51 and USGS52 nitrous oxide reference gases and perspectives on calibration needs (*Rapid Commun Mass Spectrom.* 2018;32(15):1207-1214, 10.1002/rcm.8157). *Rapid Commun Mass Spectrom.* 2018;32(20):1829-1830. doi:[10.1002/rcm.8257](https://doi.org/10.1002/rcm.8257)
 28. Crotwell A, Lee H, Steinbacher M. 20th WMO/IAEA Meeting on Carbon Dioxide, Other Greenhouse Gases and Related Measurement Techniques (GGMT-2019). Geneva, Switzerland: World Meteorological Organization; 2020.
 29. Brand WA, Coplen TB, Vogl J, Rosner M, Prohaska T. Assessment of international reference materials for isotope-ratio analysis (IUPAC technical report). *Pure Appl Chem.* 2014;86(3):425-467. doi:[10.1515/pac-2013-1023](https://doi.org/10.1515/pac-2013-1023)
 30. Gentile N, Rossi MJ, Delémont O, Siegwolf RTW. $\delta^{15}\text{N}$ measurement of organic and inorganic substances by EA-IRMS: A speciation-dependent procedure. *Anal Bioanal Chem.* 2013;405(1):159-176. doi:[10.1007/s00216-012-6471-z](https://doi.org/10.1007/s00216-012-6471-z)
 31. Liu D, Fang Y, Tu Y, Pan Y. Chemical method for nitrogen isotopic analysis of ammonium at natural abundance. *Anal Chem.* 2014;86(8):3787-3792. doi:[10.1021/ac403756u](https://doi.org/10.1021/ac403756u)
 32. Casciotti KL, Sigman DM, Hastings MG, Böhlke JK, Hilkert A. Measurement of the oxygen isotopic composition of nitrate in seawater and freshwater using the denitrifier method. *Anal Chem.* 2002;74(19):4905-4912. doi:[10.1021/ac020113w](https://doi.org/10.1021/ac020113w)
 33. Sigman DM, Casciotti KL, Andreani M, Barford C, Galanter M, Böhlke JK. A bacterial method for the nitrogen isotopic analysis of nitrate in seawater and freshwater. *Anal Chem.* 2001;73(17):4145-4153. doi:[10.1021/ac010088e](https://doi.org/10.1021/ac010088e)
 34. Felix DJ, Elliott EM, Gish TJ, McConnell LL, Shaw SL. Characterizing the isotopic composition of atmospheric ammonia emission sources using passive samplers and a combined oxidation-bacterial denitrifier approach. *Rapid Commun Mass Spectrom.* 2013;27(20):2239-2246. doi:[10.1002/rcm.6679](https://doi.org/10.1002/rcm.6679)
 35. Lachouani P, Frank AH, Wanek W. A suite of sensitive chemical methods to determine the $\delta^{15}\text{N}$ of ammonium, nitrate and total dissolved N in soil extracts. *Rapid Commun Mass Spectrom.* 2010;24(24):3615-3623. doi:[10.1002/rcm.4798](https://doi.org/10.1002/rcm.4798)
 36. Knowles R, Blackburn TH. *Nitrogen Isotope Techniques*. Academic Press; 1993.
 37. Amberger A, Schmidt HL. Natürliche Isotopengehalte von Nitrat als Indikatoren für dessen Herkunft. *Geochim Cosmochim Acta.* 1987;51(10):2699-2705. doi:[10.1016/0016-7037\(87\)90150-5](https://doi.org/10.1016/0016-7037(87)90150-5)
 38. Böttcher J, Strebel O, Voerkelius S, Schmidt HL. Using isotope fractionation of nitrate-nitrogen and nitrate-oxygen for evaluation of microbial denitrification in a sandy aquifer. *J Hydrol.* 1990;114(3-4):413-424. doi:[10.1016/0022-1694\(90\)90068-9](https://doi.org/10.1016/0022-1694(90)90068-9)
 39. York D, Evensen NM, Martínez ML, De Basabe DJ. Unified equations for the slope, intercept, and standard errors of the best straight line. *Am J Physiol.* 2004;72(3):367-375. doi:[10.1119/1.1632486](https://doi.org/10.1119/1.1632486)
 40. Cantrell CA. Technical note: Review of methods for linear least-squares fitting of data and application to atmospheric chemistry problems. *Atmospheric Chem Phys.* 2008;8(17):5477-5487. doi:[10.5194/acp-8-5477-2008](https://doi.org/10.5194/acp-8-5477-2008)
 41. Guillevis M, Vollmer MK, Wyss SA, et al. Dynamic-gravimetric preparation of metrologically traceable primary calibration standards for halogenated greenhouse gases. *Atmos Meas Tech.* 2018;11(6):3351-3372. doi:[10.5194/amt-11-3351-2018](https://doi.org/10.5194/amt-11-3351-2018)
 42. Cox MG. The evaluation of key comparison data. *Metrologia.* 2002;39(6):589-595. doi:[10.1088/0026-1394/39/6/10](https://doi.org/10.1088/0026-1394/39/6/10)
 43. Szabó ZG, Hollós E, Trompler J. Thermal decomposition of ammonium nitrate without side-reactions. *Z Phys Chem.* 1985;144(144):187-193. doi:[10.1524/zpch.1985.144.144.187](https://doi.org/10.1524/zpch.1985.144.144.187)
 44. Mohn J, Werner RA, Buchmann B, Emmenegger L. High-precision $\delta^{13}\text{CO}_2$ analysis by FTIR spectroscopy using a novel calibration strategy. *J Mol Struct.* 2007;834-836(SPEC. ISS):95-101. doi:[10.1016/j.molstruc.2006.09.024](https://doi.org/10.1016/j.molstruc.2006.09.024)
 45. Heil J, Wolf B, Brueggemann N, et al. Site-specific ^{15}N isotopic signatures of abiotically produced N_2O . *Geochim Cosmochim Acta.* 2014;139:72-82. doi:[10.1016/j.gca.2014.04.037](https://doi.org/10.1016/j.gca.2014.04.037)
 46. Sperlich P, Moossen H, Geilmann H, et al. A robust method for direct calibration of isotope ratios in gases against liquid/solid reference materials, including a laboratory comparison for $\delta^{13}\text{C}-\text{CH}_4$. *Rapid Commun Mass Spectrom.* 2021;35(1):e8944 doi:[10.1002/rcm.8944](https://doi.org/10.1002/rcm.8944)
 47. Kaiser J, Röckmann T. Correction of mass spectrometric isotope ratio measurements for isobaric isotopologues of O_2 , CO , CO_2 , N_2O and SO_2 . *Rapid Commun Mass Spectrom.* 2008;22(24):3997-4008. doi:[10.1002/rcm.3821](https://doi.org/10.1002/rcm.3821)
 48. Kaiser J. Reformulated ^{17}O correction of mass spectrometric stable isotope measurements in carbon dioxide and a critical appraisal of historic 'absolute' carbon and oxygen isotope ratios. *Geochim Cosmochim Acta.* 2008;72(5):1312-1334. doi:[10.1016/j.gca.2007.12.011](https://doi.org/10.1016/j.gca.2007.12.011)
 49. Kaiser J, Hastings MG, Houlton BZ, Röckmann T, Sigman DM. Triple oxygen isotope analysis of nitrate using the denitrifier method and thermal decomposition of N_2O . *Anal Chem.* 2007;79(2):599-607. doi:[10.1021/ac061022s](https://doi.org/10.1021/ac061022s)
 50. Kaiser J, Röckmann T, Brenninkmeijer CAM. Complete and accurate mass spectrometric isotope analysis of tropospheric nitrous oxide. *J Geophys Res.* 2003;108(15): doi:[10.1029/2003JD003613](https://doi.org/10.1029/2003JD003613)
 51. Kaiser J, Brenninkmeijer CAM, Röckmann T. Intramolecular ^{15}N and ^{18}O fractionation in the reaction of N_2O with $\text{O}(^1\text{D})$ and its implications for the stratospheric N_2O isotope signature. *J Geophys Res Atmos.* 2002;107(14): doi:[10.1029/2001JD001506](https://doi.org/10.1029/2001JD001506)
 52. Silva SR, Kendall C, Wilkison DH, Ziegler AC, Chang CCY, Avanzino RJ. A new method for collection of nitrate from fresh water and the analysis of nitrogen and oxygen isotope ratios. *J Hydrol.* 2000;228(1-2):22-36. doi:[10.1016/S0022-1694\(99\)00205-X](https://doi.org/10.1016/S0022-1694(99)00205-X)
 53. Brower KR, Oxley JC, Tewari M. Evidence for homolytic decomposition of ammonium nitrate at high temperature. *J Phys Chem.* 1989;93(10):4029-4033. doi:[10.1021/j100347a033](https://doi.org/10.1021/j100347a033)
 54. Kantnerová K, Yu L, Zindel D, et al. First investigation and absolute calibration of clumped isotopes in N_2O by mid-infrared laser spectroscopy. *Rapid Commun Mass Spectrom.* 2020;34(15):e8836. doi:[10.1002/rcm.8836](https://doi.org/10.1002/rcm.8836)
 55. Hill-Pearce RE, Hillier A, Webber EM, et al. Characterisation of gas reference materials for underpinning atmospheric measurements of stable isotopes of nitrous oxide. *Atmos Meas Tech.* 2021;14(8):5447-5458. doi:[10.5194/amt-14-5447-2021](https://doi.org/10.5194/amt-14-5447-2021)

SUPPORTING INFORMATION

Additional supporting information may be found in the online version of the article at the publisher's website.

How to cite this article: Mohn J, Biasi C, Bodé S, et al. Isotopically characterised N_2O reference materials for use as community standards. *Rapid Commun Mass Spectrom.* 2022; 36(13):e9296. doi:[10.1002/rcm.9296](https://doi.org/10.1002/rcm.9296)